Experimental Investigation of Composite Pressure Vessel Performance and Joint Stiffness for Pyramid and Inverted Pyramid Joints

By

Joseph M. Verhage

NASA/Marshall Space Flight Center

And

Mark V. Bower, Ph. D., P. E.*

The University of Alabama in Huntsville

*Corresponding Author Mailing Address:

Department of Mechanical and Aerospace Engineering

N269 Technology Hall

The University of Alabama in Huntsville

Huntsville, Alabama 35899

Phone: 256-824-6877

Fax: 256-824-7412

Email: mbower@eb.uah.edu

INTRODUCTION

The development of advanced space transportation vehicles for the next generation of launch systems will require large-scale composite pressure vessels for use as fuel and oxidizer tanks. These large-scale composite pressure vessels present a new set of technical challenges due to their size. The typical fabrication techniques used for composite pressure vessels is filament winding with an autoclave or hydroclave cure. The size of the pressure vessels produced by this technique is limited by the size of the filament winding machine and auto/hydroclave available. The large-scale pressure vessels needed for the advanced space transportation vehicles demand a new production method. One solution that has been proposed is fabrication of a pressure vessel by joining filament wound components.

This research is focused on filament wound pressure vessels with adhesive joints. This research addresses the suitability of classical laminate theory analysis tools for filament wound pressure vessels and the performance different configurations of adhesive joints used to join these systems. Specifically, this research investigates the performance of sub-scale filament wound pressure vessels fabricated of graphite epoxy with pre-impregnated (prepreg) resin tape laid adhesive joints. The suitability investigation was directed toward the structural performance of the filament wound pressure vessel wall acreage (that part of the pressure vessel that is the large cylindrical area away from the joints and unchanging in cross section), the stiffness verification of the different joint configurations and the use of industry standard failure criteria. The pressure

vessels in this study were filament wound and with two main barrel components joined by a double strap butt joint. Two different types of double strap butt joints were used in this research. They are the pyramid style and the inverted pyramid style.

The scope of this investigation was limited by programmatic and practical considerations. The restrictions include composite material selection, joint geometry, pressure vessel fabrication technique, and test requirement parameters. The composite material selected was a polymer matrix composite, specifically IM7/N5555. This material was used for all composite fabrication processes. Experimental restrictions included testing at an ambient environment with hydrostatic internal pressure and no external mechanical loads.

LITERATURE REVIEW

The structural performance of filament wound pressure vessels and its relationship to the failure mode is important part of this study. Azzam, Muhammad, Mokhtar and Kolkailah [1] discussed predesign evaluation and a potential failure path for a filament wound composite pressure vessel during an ultimate or failure pressure test. They also address the failure sequence of filament wound pressure vessels. They identified two failure sequences: the well-known first ply failure (FPF) technique and the matrix failure pressure. Uemura and Fukunaga [2] presented results from an investigation of the use of classical laminate theory for analysis of filament wound cylinders and the use of the Tsai-Wu failure criteria to predict the failure pressure. Lifshitz and Dayan [3] addressed the process for calculating the stresses and strains in non-symmetric

filament wound pressure vessels with thick metal liners. The prediction calculations of this study were based on classical laminate theory and the Tsai-Wu failure criterion. An important conclusion of this paper, which relates to this study, is that *in situ* measurements of mechanical properties of filament wound vessels are needed in order to determine moduli and strength values. They observed that these properties are not the same as those obtained from unidirectional laminae testing. Kam, Liu, and Lee [4] presented the results of an investigation of the first-ply failure strength of laminated composite pressure vessels. The failure criteria used in this paper included the Maximum strain, Maximum stress, Hoffman, Tsai-Hill and Tsai-Wu. This study revealed that for composite pressure vessels composed of eight plies there exists significant differences (20% and greater) between the theoretical and experimental first-ply failure pressures.

Chamis and Murthy [5] showed the use of simplified procedures for designing adhesively bonded composite joints. They used the shear lag equations to calculate the key strength property values for their study. Mitra and Ghosh [6] addressed the importance of interfacial stresses and the load transfer of load between the adherend and joint. They investigated the deformation behavior of the double strap butt joint under a tension load and how the deformation affects the failure mode of the joint. Ahn and Springer [7] presented analytical and experimental results for the strength of repaired areas of composite laminates. The article presents information on the relationship between the number of external stepped lap plies and the failure load for the repaired area. They

observed that the addition of external plies, which cover all the subsequent plies of the scarf repair, increases the failure load in comparison to scarf joints without external plies. The scarf joint with external plies is similar to the inverted pyramid joint configuration of this study.

BACKGROUND THEORY

The elements of classical laminated plate theory are well-known and well documented in any number of excellent texts on composite materials. To conserve space the background details are left to the interested reader. We find for a laminated composite pressure vessel, that the mid-plane strain can be expressed in terms of the pressure in the vessel as:

$$\varepsilon_1^o = (\frac{a_{11}D}{4} + \frac{a_{12}D}{2})P \tag{1}$$

and

$$\varepsilon_2^o = (\frac{a_{12}D}{4} + \frac{a_{22}D}{2})P\,, \tag{2}$$

where the a_{ij} are the in-plane extensional compliances, D is the vessel diameter, and P is the internal pressure.

There are many different failure criteria used in industry today. For example: Maximum Stress Failure Criterion, Maximum Strain Failure Criterion, Tsai-Hill Failure Criterion, Hoffman Failure Criterion, Tsai-Wu Quadratic Tensor Polynomial Failure Criterion and the Yamada Failure Criterion. Each of these criteria has their own set of advantages and disadvantages and an evaluation of these criteria is beyond the scope of this research. This study will use the Tsai-Wu Quadratic Tensor Polynomial Failure Criterion, or more simply the Quadratic

Failure Criterion. The Quadratic Failure Criterion is a commonly accepted composite failure criterion that has been discussed widely in the literature. The Quadratic Failure Criterion, $F(\sigma)$, is:

$$F(\sigma) = \sum_{i=1}^{6} F_i \sigma_i + \sum_{j=1}^{6} \sum_{i=1}^{6} F_{ij} \sigma_i \sigma_j \tag{3}$$

where σ_i are the stresses, F_i and F_{ij} are the linear and quadratic strength coefficients, respectively. Tsai[] presents a thorough discussion of the strength coefficients and the transformation of the coefficients into structural directions. The Hahn form of F_{12} is used in this research in the Laminate computer program.

The strength ratio is used in the analysis of composite material failure as a quasi-factor of safety. The strength ratio, also known as the R factor, is a ratio of the applied stress to the stress at failure assuming that all components are scaled by the same factor. The R factors are calculated by using

$$R = \frac{\sigma_i^{\max}}{\sigma_i^{\text{applied}}} . \tag{4}$$

The R factor is substituted into the Quadratic Failure Criterion equation (3) and the function is set equal to one which gives the following relationship:

$$\left[\sum_{j=1}^{6}\sum_{i=1}^{6} F_{ij}\sigma_i\sigma_j\right] R^2 + \left[\sum_{i=1}^{6} F_i\sigma_i\right] R - 1 = 0, \tag{5}$$

from which the R factor can be determined. Based on the definition in Equation 4, the R factor can then be used to predict failure by the following rule:

$R > 1$ the laminate is structurally safe,
$R = 1$ Failure and
$R < 1$ Over loaded .

When the *R* ratio is greater than 1 it may be considered as the quasi-safety factor for the composite structure analyzed.

EXPERIMENTAL PROCEDURE

Constraints made it possible to test only one vessel or article of each joint design of a single material type. It is important to note that one joint design was used on each vessel. A single lamination scheme was used for both vessels. The vessels were 12 ply symmetrical laminates, with a stacking sequence for the vessels of $[90/60/-60/30/-30/0]_S$. The material chosen for the composite cylinders was a Hercules IM7/8552 graphite epoxy. The IM7/8552 used for the filament winding process was a prepreg carbon fiber. The material properties for IM7/8552 are listed in Table 1

The two test articles fabricated for this research study were filament wound cylinders that were cured in a standard autoclave. Both test articles were cut in half after they were fully cured. They were then reconnected with different configurations of a double strap butt joint. The two different joints that were fabricated in this study included the pyramid style joint and the inverted pyramid style joint.

The two composite bottles that were used for this experimental investigation were fabricated at the Product Enhancement Facility (PEC) at the George C. Marshall Space Flight Center in Huntsville, Alabama. The dimensions of the composite bottles used in the investigation were determined by programmatic constraints beyond the control of this investigation. The composite bottles were 45.7 cm (18 in.) in diameter, 82.6 cm (32.5 in.) from end to end with

a nominal wall thickness of 0.178 cm (0.07 in.). The fabrication process used is described in detail by Verhage [].

After the bottles were fabricated, they were cut in half in preparation for the joint layup fabrication step. Each composite bottle was cut in half at the 40.6 cm mark as measured from the top surface of the top polar boss using a lathe type fixture with a precision diamond saw. The two halves of each bottle were dry fit on the inflatable mandrel to measure the maximum gap between the two halves. The tank halves were marked for realignment on the inflatable mandrel after the joint surface preparation was complete.

The surface preparation of the tank wall is critical to the adhesive bond strength of the joint. The next step required that the inside surface of both halves be grit blasted and cleaned with acetone in a region measuring 6.35 cm from the edge of the cut around the circumference of the bottle. After the joint surface preparation was complete, the two halves of the bottle were reinstalled on the inflatable mandrel. Hysol EA9394 epoxy adhesive was applied on the butt joint area and the bottle halves were pushed together and the alignment was verified. The EA9394 epoxy adhesive was allowed to cure for 24 hours in an ambient environment. Once the epoxy adhesive cure was complete, the outer joint surface was grit blasted and cleaned with acetone in a region measuring 6.35 cm on both sides of the cut. With the surface preparation complete the following steps were performed to complete the joint fabrication.

1. Outer Joint Fabrication Process

- Lay one 10.2 cm wide ply of FM300-2K film adhesive centered at the butt joint
- Bag joint region with film adhesive and debulk for 15 minutes

- Remove the bag
- Lay a ply of IM7/8552 around the circumference, stagger seams of each ply by 60°
- After 3 plies of IM7/8552 have been laid, bag and debulk for at least 30 minutes
- Remove the bag
- Lay remaining 3 plies of IM7/8552 and debulk for at least 30 minutes
- Bag outer joint region for oven cure

2. Inner Joint Fabrication Process

The inner joint surface preparation and ply layup sequence was done similar to the outer joint. The stacking sequence, material and fiber orientation of each ply for the two different joint configurations are shown in Tables 2 and 3. Note in these tables that the only difference between the bottles is the width of the layers.

The orientation of each ply in the joint laminate for each composite cylinder is as follows: $[90/60/-60/30/-30/0/\text{Tank Wall}/0/-30/30/-60/60/90]_T$. Consequently, the laminate classification shows a 24-ply laminate joint. It is important to note that the total joint makeup contains both a filament wound laminate (tank wall) and two tape laid laminates on each side of the tank wall. Consequently, the joint structure is a mixture of filament wound and laminated plies.

Composite bottle #1 used a pyramid style joint layup with the widest composite ply as the first strap ply adjacent to the butt seam. Each subsequent ply applied was 1.27 cm narrower in width with the all the ply widths ranging from 8.89 cm to 2.54 cm. Composite bottle #2 used an inverted pyramid style joint

layup with the narrowest ply as the first ply adjacent to the seam. Each subsequent ply applied was 12.7 cm wider than the previous with the ply widths ranging from 2.54 cm to 8.89 cm with the outermost strap ply completely overlapping and enveloping the plies beneath it. The Figures 4 and 5 show the laminate stacking sequence and ply orientations for both the tank wall of the composite cylinders and the corresponding joint configuration and its associated orientation.

Test Plan and Methodology

The test plan for the experimental investigation portion of this study required that several objectives be met during the test activities. The objectives include: recording test data from the required instrumentation, hydrostatically test the composite cylinder to the required pressures, and investigate the failure mode and pressure of each composite test article. The results from the tests provided data for the analysis phase of the investigation of the joint strength and pressure vessel performance for the two different joint designs. The test data recorded from the test operations were processed and compared to the analytical predictions generated by computer programs discussed in the following chapter. The test fixtures and facilities were provided by the Structural Strength Test Team of the NASA, Marshall Space Flight Center. A complete description of the test fixtures, hydrostatic pressurization system, ant test article setup is included in Verhage[]. The test article and fixture setup is shown in Figure 8.

A complete and detailed description of the test article instrumentation and data acquisition system is presented by Verhage[]. As noted above the test

requirements include recording various information items during the tests. The information to be recorded for each test includes: strains at multiple locations on and in the pressure vessels, the applied internal pressure, deflection at points on the vessels, and video of the test. The strain data was obtained using strain gages with the deflection data obtained from 10-volt transducers. The strain and deflection instrumentation on each of the two composite bottles consisted of ten biaxial strain gages and ten deflection measurement points.

The measurement acquisition hardware used in this investigation is based on a Personal Computer (PC) class system with a remote data harvester (RDH) and display unit. The remote data harvester receives the analog output from the instrumentation and performs an analog to digital conversion with signal conditioning. The conditioned digital output goes to the PC-based unit. The PC is the central data processing unit in the system, which operates with a Windows software environment. The digital signals are recorded and converted into engineering units and displayed in real time for the test operator. All test data in these tests was sampled and recorded at one record every 250 milliseconds or 4 data points per second.

A video system was used to record each test of the vessels. The video system incorporates a precision time stamp on each image, which allows for correlation of the video to the test data record.

The Test Requirements for this program specified three test conditions to ascertain the following: No Leakage, Influence Reference for Leak Checks, Design Limit Load, and Ultimate Load. Three test conditions to achieve these

requirements were planned in the following sequence: Influence Reference for Leak Checks accomplished in Test Condition 1, Design Limit Load (300psig) accomplished in Test Condition 2, and Ultimate Load (Failure) accomplished in Test Condition 3. The details of test procedures are omitted to conserve space. They are presented in Verhage[]. During the tests on the pyramid joint pressure vessel the test pressure exceeded the safety valve pressure. The safety valve was subsequently removed and Test Condition 3 repeated for the pyramid joint vessel. Consequently, there are two performance tests for the pyramid joint. The safety valve was not reinstalled for the inverted pyramid joint test.

ANALYTICAL PROCEDURES

The use of computer programs for structural analysis of composite materials is commonplace in the development of new structures and the redesign of older structures. Computer software was used in this research to derive the necessary analytical values for comparison to experimental data. Two computer analysis programs, which utilize the classical laminate theory derivations discussed previously, were used in this study. The use of two programs provided a crosscheck process for the results. This crosscheck in derivations helped minimize the error in the research process. These two computer programs were used for analysis on both the tank wall and joint for each composite pressure vessel. The analysis procedure for the two computer programs were somewhat different due to the diversity of operating systems used to execute the programs. One of the computer analysis programs used was a Microsoft Excel® based program with macros developed and written by Dr. Mark V. Bower of the

University of Alabama in Huntsville. This computer program is referred to as Laminate in this study. The second computer program was a Microsoft DOS based program written by Peter Sjoblom from the University of Dayton and sold by Think Composites. This computer program is referred to as GENLAM in this study. A detailed discussion of the use of each of these programs is presented in Verhage[].

RESULTS

B. Tank Wall Performance

The investigation of the tank wall performance was a key step in understanding the accuracy of the classical laminate theory in predicting the structural behavior of the filament wound system. The strain data and the associated analysis are presented in the following subsection. The deflection data from the tests is reported by Verhage[].

3. Strain Results

The tank wall was analyzed as a 12 ply laminate although the tank wall fabrication technique for this study was filament winding. The approach used to investigate the tank wall performance started with recording the strain gage data from both composite pressure vessels. The inner and outer strain values of back-to-back strain gages were averaged to obtain the mid-plane strain value. Plots of the mid-plane strain results for both the axial and hoop directions are shown in Figures 4 and 5. These plots show the test pressure versus the mid-plane strain values for the tank wall for both the pyramid and inverted pyramid test articles as measured above and below the joint. Due to the similarity in the strain results

between the first and second pyramid joint test runs, only values from the first pyramid joint test run and the inverted pyramid joint test are plotted to show the mid-plane strain results.

In the analysis of the experimental results the first observation made is that there is a strong correlation between the strain, both axial and hoop, measured at the top location (above the joint) for both joint configurations, see Figures 4 and 5. The second observation is that there is a strong correlation between the strains, both axial and hoop, measured at the top (above the joint) and bottom (below the joint) locations. However, the strains measured at the bottom location are slightly above those measured at the top for all test configurations. From these observations we conclude that: there is repeatability in the data, the measurement locations in the tank wall acreage are sufficiently far away from the joint that the joint behavior does not significantly affect the results, and there may be a small systematic difference in the loading between the top and bottom locations. The weight of the water used to fill the tank and the associated pressure gradient may account for this small difference.

The next part of the tank wall performance investigation was to compute pressure values from the mid-plane strains for the pressure load profile until failure. The generation of pressure values was accomplished by entering the experimental mid-plane strain values shown in the previous plots into the GENLAM and Laminate computer programs. The computer programs generated stress resultant values to be used to calculate the analytical pressure profile. The stress resultants in the axial direction were used with the pressure vessel

equations, Equations 1 and 2, to calculate the analytical pressure values. After the analytical pressure values were calculated, they were compared to the test pressure values recorded from the pressure transducer used on the test setup. The comparison of the analytical versus experimental pressure values is shown in the plots in Figure 6 through 11. This comparison also corresponds to both the top and bottom sections of the tank wall.

The results shown in Figures 6 through 11 reveal that the test pressure data points from the pressure transducer falls on the analytical pressure curves for the top strain gages. These results support the conclusion that the classical laminate theory computer programs predict the structural performance of filament wound systems within a ±5% accuracy range. The tank wall performance results provide the validation for the use of classical laminate theory to analyze the structural performance of the filament wound systems with acceptable accuracy.

C. Joint Stiffness Verification

The joint stiffness verification was the next area of focus. The computer programs were used to generate the extensional stiffness values for the two different joint configurations. As previously stated the two different joint configurations were 24 ply symmetrical laminates consisting of a combination of filament windings and prepreg tape. The analytical extensional stiffness matrix $[A]$ along with the extensional compliance stiffness matrix $[a]$ were the same for each of the two joint configurations. This was the case because the two joint configurations were analyzed using the same stacking sequence and material properties. The extensional compliance stiffness and analytical force resultants

were used to calculate the analytical mid-plane strains. The analytical mid-plane strains are plotted on a pressure versus strain curve in Figures 12 and 13. The axial direction joint stiffness plot shown in Figure 12 presents the analytical curve versus the test data curves. The circumferential data plot, shown in Figure 13, shows the original theoretical curve and an adjusted analytical curve versus the test data curves.

The results shown in Figures 12 and 13 show that the stiffness prediction for the joints in the axial direction is within a 2 to 5% accuracy range without any adjustment ratio applied. The analytical curve in Figure 12 predicts a slightly stiffer structure in the axial direction compared to the test data results. The joint stiffness results in Figure 13 for the circumferential direction reveals that the original analytical curve predicts a much less stiff structure than the test data results show. During the tank wall performance, which is the first part of this investigation, it was noted that the analytical circumferential stress resultants generated by the computer programs were around 25% less than the calculated theoretical results. The following tables (P1, P2 and IP1) show the calculated average of the stress resultant ratio of the theoretical value divided by computer generated value. The stress resultants in these tables were in relation to the tank wall acreage.

Tables 6.1 through 6.3 clearly show that the computer program generated stress resultants in the axial direction are only 1% less than the theoretical value. Tables 6.1 through 6.3 also clearly show that the computer program generated stress resultant values in the hoop direction are 25% less than the theoretical

value. The 25% was applied to the circumferential joint stiffness results as a correction factor by dividing the N_2 value by 1.25 to decrease the stiffness slope of the original theoretical mid-plane curve. After the 1.25 correction factor was applied, the curve rotated and fell within a 5 to 10% error range in relation to the experimental curves. With the application of strain gages on composite materials, this is an acceptable range[i]. The correction factor was only applied to the hoop mid-plane strain equation for both pressure vessel data results and successfully produced a stiffness prediction curve for the different joint configurations. The joint stiffness verification plots are as follows.

D. Failure Criteria

The final part of this study consisted of analyzing the failure of the filament wound pressure vessels using the Quadratic Failure Criteria. The quadratic failure analysis was derived using the GENLAM and Laminate computer programs. The failure analysis produced a minimum strength ratio value R to be 8.85 for a 100-psig test case. This indicates a first ply failure (FPF) of 885 psig for ply layers 6 and 7, which are the 0° laminae in the middle of the laminate. The analysis also predicted a last ply failure or burst of 949 psig with the plies 1 and 10 the last laminae to fail. Plies 1 and 10 of the laminate were stacked at 90°.

[i] Interview with NASA Instrumentation Engineer Houston Hammac, P.E.

1. Inverted Pyramid Pressure Vessel

With regard to the test results, the filament wound pressure vessel with the inverted pyramid joint configuration failed at 850psig, which is 10.4% below the actual predicted failure of 949psig generated from the computer programs. In Figure 5.11 still frame pictures taken from recorded video shows the failure mode for the IP1 test run.

Frame B shown above reveals that the test article ruptured in the tank wall acreage at the bottom of the tank and Frame C shows that the pressure vessel did not separate in pieces at the joint. At the initial failure, Frame B shows the water exiting at the tank wall area rather than the joint area. The video frames, test data and computer analysis in combination show that the inverted pyramid test article failed in the tank wall acreage and not at the joint. Recall further that the strain gages at the bottom of the tank had higher strains due to the weight of the water in the tank. This accounts for the failure beginning at the bottom of the tank and may account for the disagreement between the predicted and actual value.

2. Pyramid Joint Pressure Vessel

The filament wound pressure vessel with the pyramid joint configuration failed at 630psig, which is 33.6% below the predicted failure of 949psig generated by the computer programs. The still pictures or frames taken from the recorded video for the pyramid joint pressure vessel are shown in Figure 5.12. These pictures show the failure mode of the P2 test run.

Frame B in Figure 5.12 shows the force of the water at failure exiting around the midsection of the tank, which is the area of the joint. After failure,

Frame C in Figure 5.12 shows a top portion of the pressure vessel separated at the joint section. Another camera view from the P2 test run also reinforces the previous conclusions as shown in the still pictures in Figure 5.13.

Again, Figure 5.13 Frame B shows an intense white at the middle, which represents a blast of the water exiting the tank at the midsection of the pressure vessel. Frame C in Figure 5.13 shows a split at the joint area after failure. The test data resulting in a low failure pressure in combination with the recorded video reinforce the conclusion that the pressure vessel with the pyramid style joint failed at the joint. Predicting failure the mode of failure at the joint is beyond the scope of this investigation. Failure due to peel or adhesive stresses in the joint can cause the pressure vessel to burst before reaching the predicted failure of the tank wall, which is the case in the P2 test run.

3. Failure Analysis Comment

It should be noted here that the predictions that the tank wall was the failure origin for the Inverted Pyramid Joint vessel and that the joint was the failure origin for the Pyramid Joint vessel were made based on the analysis results and subsequently confirmed by review of the video recordings. This adds credibility to the analytical method used in this investigation.

CONCLUSIONS, RECOMMENDATIONS AND FUTURE WORK

The investigation of the tank wall acreage performance was a critical step in assessing the correlation of the experimental structural behavior with the analytical structural predictions for the filament wound pressure vessels. After reviewing the generated stress resultants from the experimental strain input, the

axial stress resultant showed a strong correlation with the theoretically calculated values from the mechanics of material equations for pressure vessels. When the computer generated hoop stress resultant values were reviewed they were an average of 25% less than the theoretically calculated values from mechanics of material equations. The 25% lag in stress magnitude was consistent throughout the range of the tests for each filament wound pressure vessel. Based on this information it is concluded that the analytical calculations overestimate the stresses in the hoop direction by 25%. This factor was used subsequently in the joint and failure analysis for the vessels. While it is reasonable to apply this factor in this investigation, because it is self-consistent, this factor may not apply to all filament wound pressure vessels. It is likely that this factor is dependent on the number and orientation of the laminae of the vessel. It can also be concluded in relation to Lifshitz & Dayan [3] that the measurements of mechanical properties of filament wound vessels are needed in order to determine moduli and strength values, which are not the same as those obtained from unidirectional laminae.

The computer generated axial stress resultants were used to calculate the theoretical pressures and in turn compared to the experimental test pressures for verification of structural performance of the filament wound pressure vessels. In this part of the study it can be concluded that by using the axial stress resultant value the classical laminate theory can accurately predict the structural performance of the tank wall laminate in a filament wound pressure vessel with different joint configurations.

The joint stiffness verification study involved two different joint laminate configurations. The geometry of the joints was different but they had the same number of plies, angle stacking sequence and thickness. Consequently, the extensional compliance matrices were the same for both configurations. The analytical stiffness curve for the axial direction showed a strong correlation with the experimental stiffness curves for the two different joint configurations. Differences between the analytical and experimental results are well within the experimental error. Consequently, it is concluded that the axial response of either a pyramid or inverted pyramid joint can be modeled accurately by classical laminate theory. The analytical stiffness curve for the hoop direction under predicted the stiffness in the joint when compared to the experimental stiffness curves for the two different joint configurations. As was observed in the tank wall acreage comparison, the average error in the hoop stress resultants was 25%. When the analytical calculations for the hoop mid-plane strains were adjusted by a correction factor of 1.25 on the hoop stress resultant there was good agreement between the modified analytical results and the experimental results. The agreement between the modified analytical results and the experimental results is well within the experimental error. This correction factor is consistent with the adjustment needed for agreement between the analytical and experimental results in the tank wall acreage. Again, the correction factor used here is self-consistent and is expected to be different for other stacking sequences. Consequently, the correction factor should be determined for each specific application. Further, it is concluded that the classical laminate theory can be used, with reasonable

accuracy, to predict the axial stiffness of different types of double butt strap joints manufactured with a combination of filament wound and prepreg tape laminae. Although, by using the classical laminate theory, the prediction of the hoop stiffness in the joints must have a correction factor applied to produce a more accurate analytical stiffness curve.

The last part of this study involved the investigation in the use of classical laminate theory failure criteria in relation to filament wound systems. The experimentally determined failure pressure for the inverted pyramid joint vessel is 10.4 % below the analytically predicted failure pressure for the tank wall acreage. From review of video from the test it is concluded that the inverted pyramid joint tank failed in the tank wall. It is then concluded that the quadratic failure criterion can provide a failure prediction that is within approximately 10% of the actual failure for filament wound pressure vessels. However, the failure prediction may be non-conservative, as in this application. The pyramid joint configuration pressure vessel failed 33.6% below the predicted failure pressure. From review of video from the test and the over prediction of the failure pressure it is concluded that the pyramid joint tank failed in the joint.

Another significant conclusion from the failure investigation was the importance of the use of video recording during the conduction of the tests. The video recording from this study provided a valuable piece of evidence to determine the failure mode of each filament wound pressure vessel. In order to make the video most effective, it is important to make sure that the data system time clock is synchronized with the video recording time clock. This time

synchronization provides an important tool when the recorded instrumentation data is combined with the failure video of the test article to create the most accurate failure evidence.

The use of the classical laminate theory in this study produced very promising results for predicting the structural performance, stiffness and failure of filament wound systems. The use of classical laminate theory computer programs provides an important tool for quickly and efficiently analyzing the structural behavior of composite materials. We can conclude that these tools can be used to analyze the structural behavior of filament wound systems such as pressure vessels.

As with most research programs or studies, additional work to extend and refine the current investigation is expected and essential. This study is no exception. Future studies of filament wound systems, especially those for the space industry, should be focused on the composite material selection, multiple joint configurations, operation environment and structural health monitoring. Some of the work in the following discussions is currently in process.

A more in depth analysis of the structural response of the pressure vessels is needed. This investigation made use of a simplified approach to predict the response and failure for the vessels in question. A greater understanding of the influence of the joint on the structural response is needed. By careful analysis of the bending moments in the structure that result from the joint, a more accurate predicted failure pressure may be achievable. Also, the failure prediction of a filament wound system with an adhesive joint may requires further investigation

of the influence of peel and adhesive stresses on the joint failure loads. A valuable addition to this investigation would be a test of filament wound pressure vessels without midsection joints. This would provide verification to the tank wall acreage analysis and provide needed insight into the affects of the joint on the structural response. Further, tests with other midsection joint configurations would provide additional understanding of the joint performance. A test program that incorporates five or more filament wound pressure vessels of each type instrumented with triaxial strain gages is needed. Five pressure vessels of each type would help establish repeatability in the data, especially in the failure criteria area. The triaxial strain gages would provide data for the in-plane shear component to be incorporated with the axial and hoop strain data. To add to the previous discussion of adding triaxial strain gages and performing a more enhanced investigation of the joint region is the ability to do deflection mapping of the overall pressure vessel. Deflection mapping would provide the stress analyst the ability to investigate the out-of-plane deflections as well as axial deflections in order to understand the deflection gradients across regions of dissimilar construction and to correlate that information with high fidelity finite element models. Along with the triaxial strain gages, additional instrumentation in the realm of fiber optics strain sensors may serve as a structural health monitoring system for cyclic loading. Also, the use of Acoustic Emissions may provide a valuable tool in the detection of the first-ply failure and help predict the failure of the filament wound pressure vessels.

An important part of any test program is to test the structure being investigated in an environment that is as close to the operational environment as is possible. A critical environmental factor for any pressure vessel that is being investigated for the use for fuel or oxidizer tanks is the cyclic loading with cryogenic temperatures and pressures. An important continuation of this study is the testing of the vessels with liquid nitrogen (LN_2) and eventually liquid hydrogen (LH_2) depending on the material compatibility and safety factors. An investigation into the micro-cracking and permeability of composite laminates under a cryogenic environment is a natural part of such a study.

Pretest and post-test nondestructive evaluation (NDE) of all future composite pressure vessels is recommended. These evaluations help detect flaws or delaminations produced during manufacturing, which then provide an explanation for differences between experiment and analysis results. NDE data is important information for testing filament wound pressure vessels with or without joints.

In relation to the previous discussion on video coverage for the conduction of tests there are several key elements that can be added to further enhance the results. There are several recommendations that may help gather more conclusive evidence. For example, high speed video or video with more enhanced shutter speeds would provide more video frames during a particular time scenario of interest. Also, the installation of cameras encased in a protective housing would provide the test requester an option to see a closer view of the pressure vessel in order to do a remote visual inspection for leaks during pressurization.

The previous recommendations and future work will enhance further investigations of composite pressure vessels. During the development and testing of new composite pressure vessels, it is critical to understand the structural behavior by using the proper combination of investigation tools such as computer analysis, instrumentation, health-monitoring systems and video.

ACKNOWLEDGEMENTS

The authors wish to express their thanks for the support of NASA/Marshall Space Flight Center in the performance of this research program.

REFERENCES

Table 1

Hercules IM7/8552 Material Properties

Property	Principal Material Direction	Symbol	Value
Tensile Modulus	First	E_1	161 GPa
Tensile Modulus	Second	E_2	11.5 GPa
Shear Modulus	In-plane	E_6	4.96 GPa
Poisson's Ratio	In-plane	ν_{12}	0.32
Maximum Tensile Strength	First	X_T	2.68 GPa
Maximum Compressive Strength	Second	X_C	1.77 GPa
Maximum Tensile Strength	First	Y_T	111 MPa
Maximum Compressive Strength	Second	Y_C	305 MPa
Maximum Shear Strength	In-plane	S	119 MPa
Coefficient of thermal expansion	First	α_1	$-0.0719\ 10^{-6}$/°C
Coefficient of thermal expansion	Second	α_2	$21.2\ 10^{-6}$/°C
Coefficient of moisture expansion	First	β_1	0.0
Coefficient of moisture expansion	Second	β_2	0.6
Cure temperature		T_{cure}	177°C
Laminae thickness		h_o	0.127 mm
Volume fraction of fiber		V_f	0.66

Table 2

Pyramid Double Butt Strap Joint Layup for both inner and outer straps

Stacking Sequence	Material	Ply Width (cm)	Fiber Orientation
Tank Wall	IM7/8552, EA9394	NA	[90/60/-60/30/-30/0]s
Layer 1	FM300-2K	10.2	NA
Layer 2	IM7/8552	8.89	[0°]
Layer 3	IM7/8552	7.62	[-30°]
Layer 4	IM7/8552	6.35	[30°]
Layer 5	IM7/8552	5.08	[-60°]
Layer 6	IM7/8552	3.81	[60°]
Layer 7	IM7/8552	2.54	[90°]

Table 3

Inverted Pyramid Double Strap Joint Layup for both inner and outer bellybands

Stacking Sequence	Material	Strap Width (cm)	Fiber Orientation
Tank Wall	IM7/8552, EA9394	NA	[90/60/-60/30/-30/0]s
Layer 1	FM300-2K	10.2	NA
Layer 2	IM7/8552	2.54	[0°]
Layer 3	IM7/8552	3.81	[-30°]
Layer 4	IM7/8552	5.08	[30°]
Layer 5	IM7/8552	6.35	[-60°]
Layer 6	IM7/8552	7.62	[60°]
Layer 7	IM7/8552	8.89	[90°]

Table 4

Summary of Stress Resultant Ratios for Tank Wall

		N_1 Ratio			
		GENLAM		Laminate	
		Average	Standard Deviation	Average	Standard Deviation
Pyramid Style Joint	Test 1	1.01	0.0416	0.97	0.0116
	Test 2	1.05	0.0487	1.02	0.0206
Inverted Pyramid Style Joint		1.02	0.0326	0.99	0.0091
		N_2 Ratio			
		GENLAM		Laminate	
		Average	Standard Deviation	Average	Standard Deviation
Pyramid Style Joint	Test 1	1.24	0.0116	1.21	0.0144
	Test 2	1.27	0.0332	1.24	0.0411
Inverted Pyramid Style Joint		1.23	0.0187	1.21	0.0174

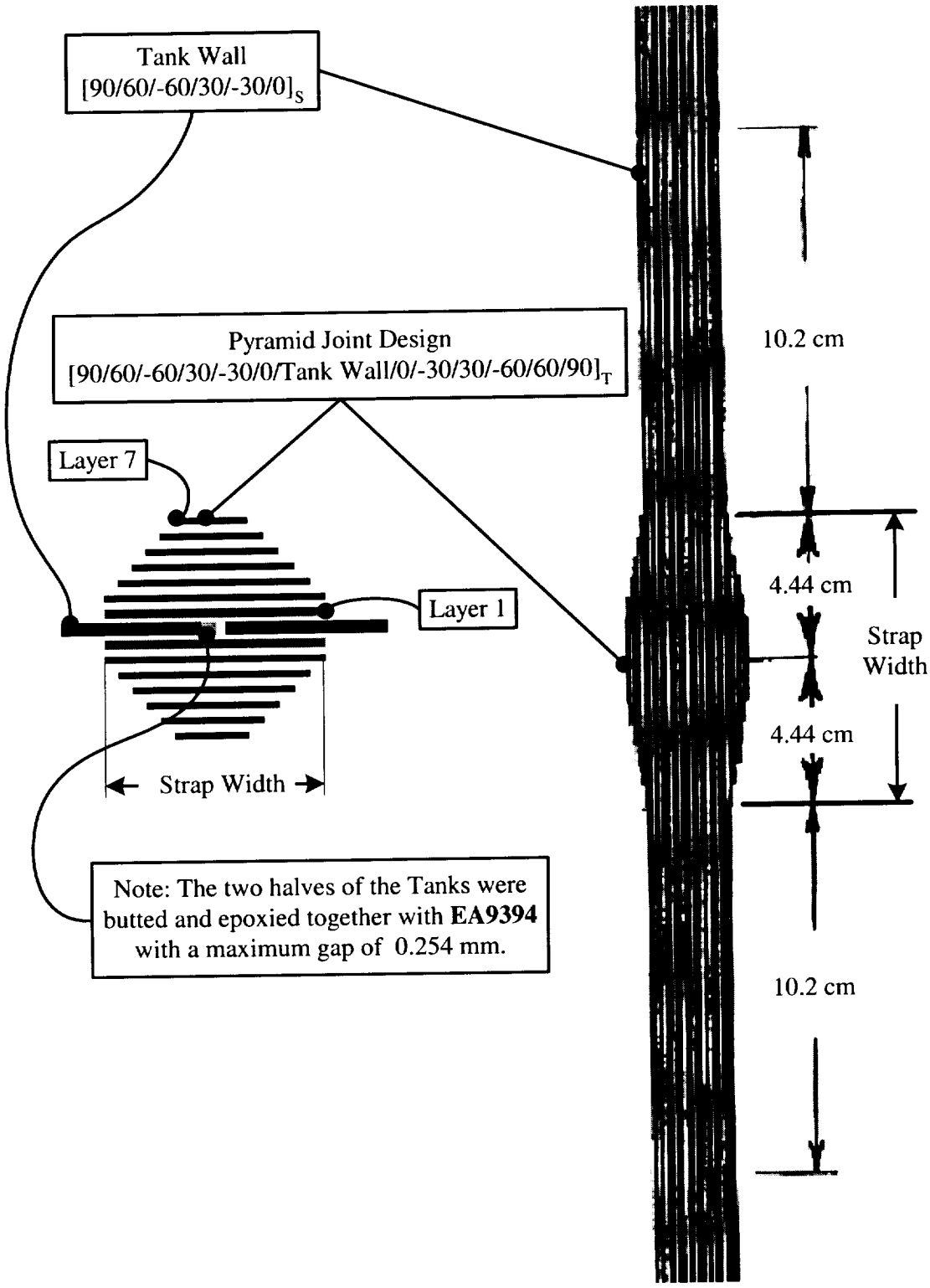

Figure 1 Pyramid Double Strap Joint Design

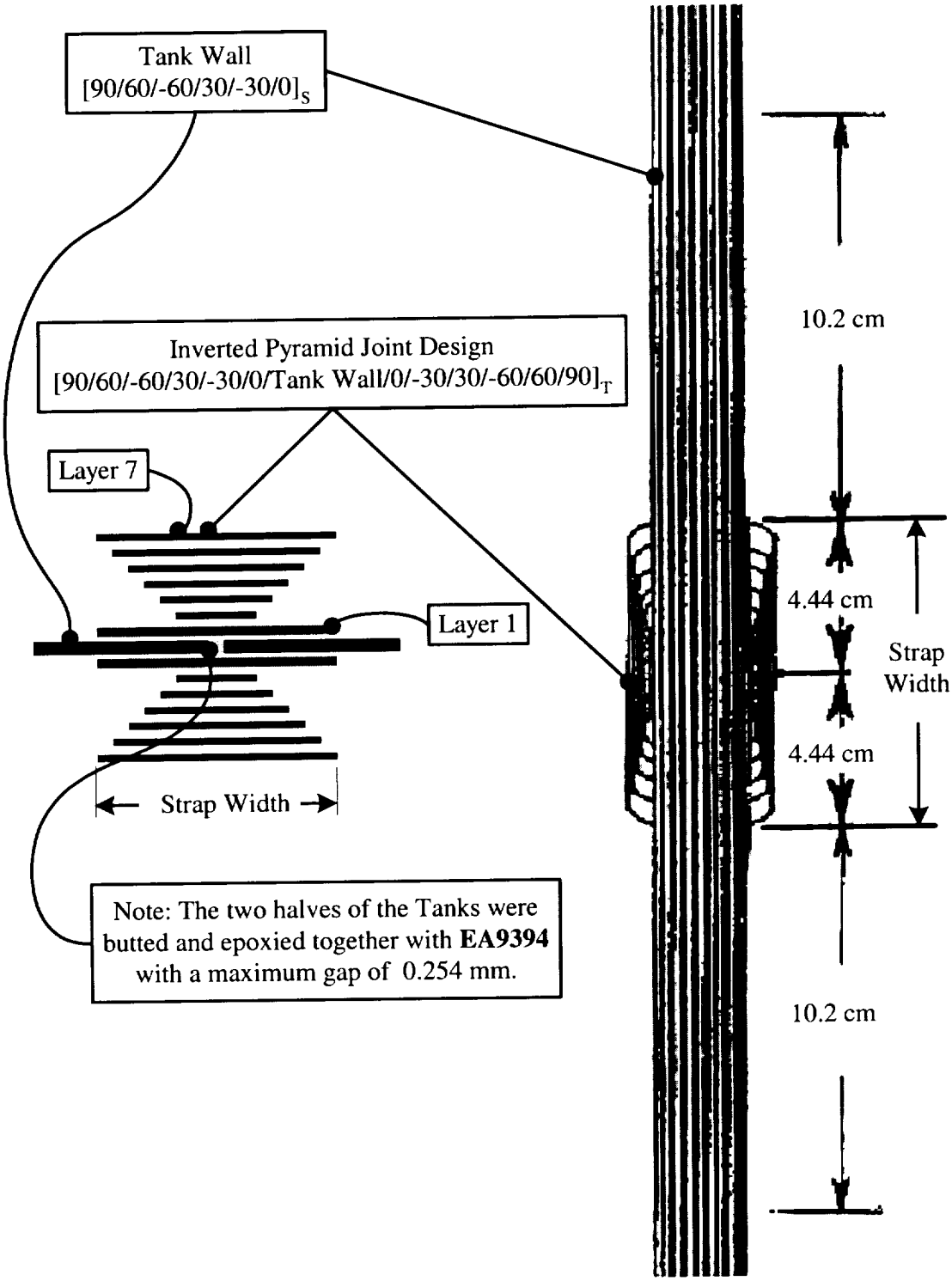

Figure 2 Inverted Pyramid Double Strap Joint Design

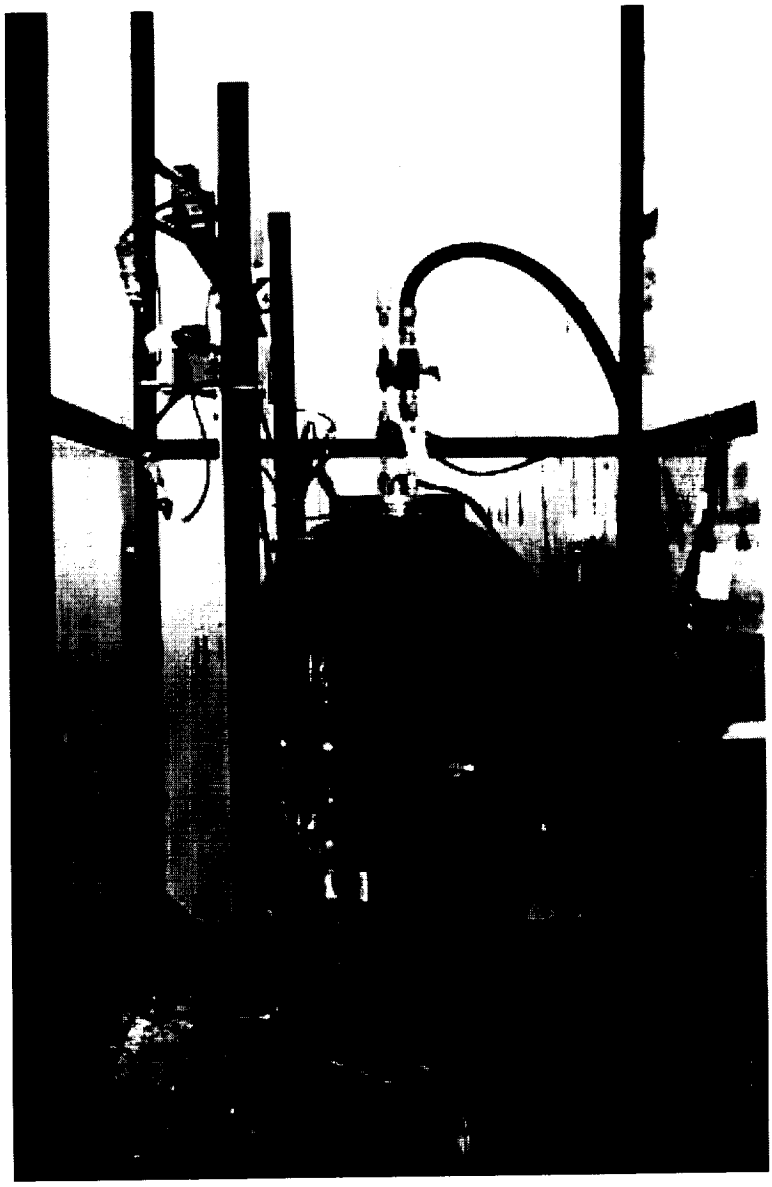

Figure 3 Test Setup of Composite Pressure Vessel and Fixtures in Safety Booth

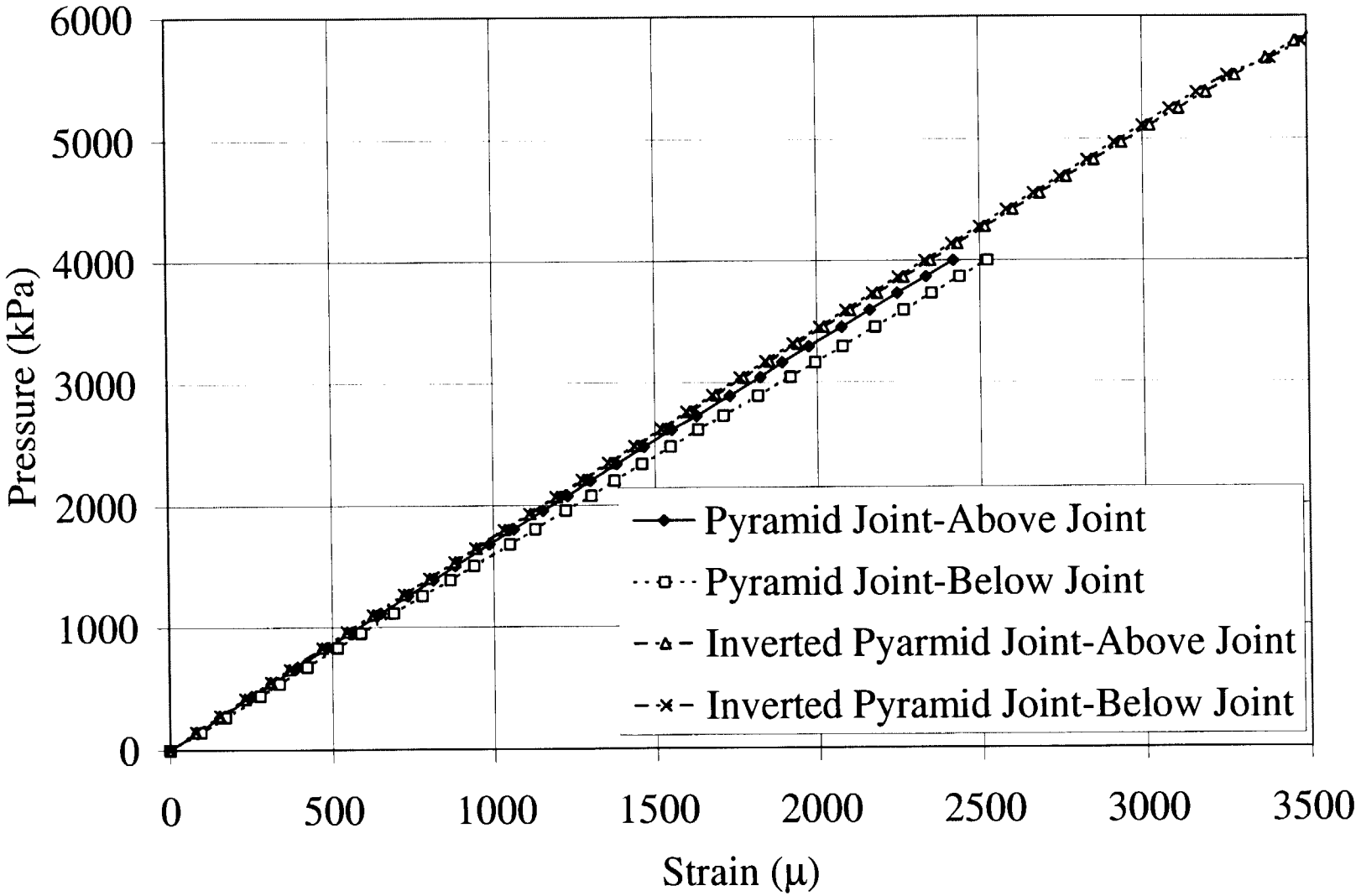

Figure 4 Mid-plane Axial Strains for Tank Wall

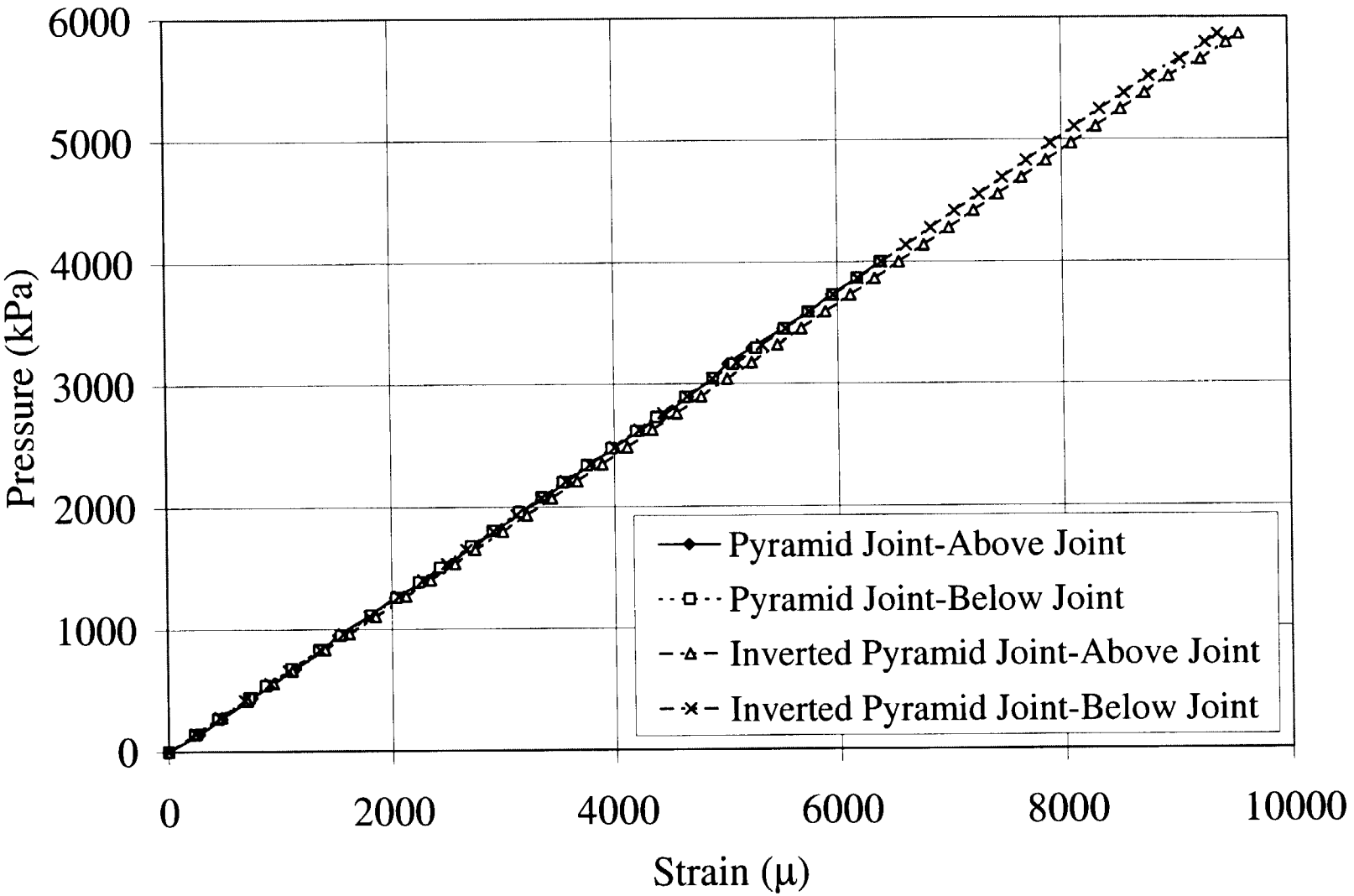

Figure 5 Mid-plane Hoop Strains for Tank Wall

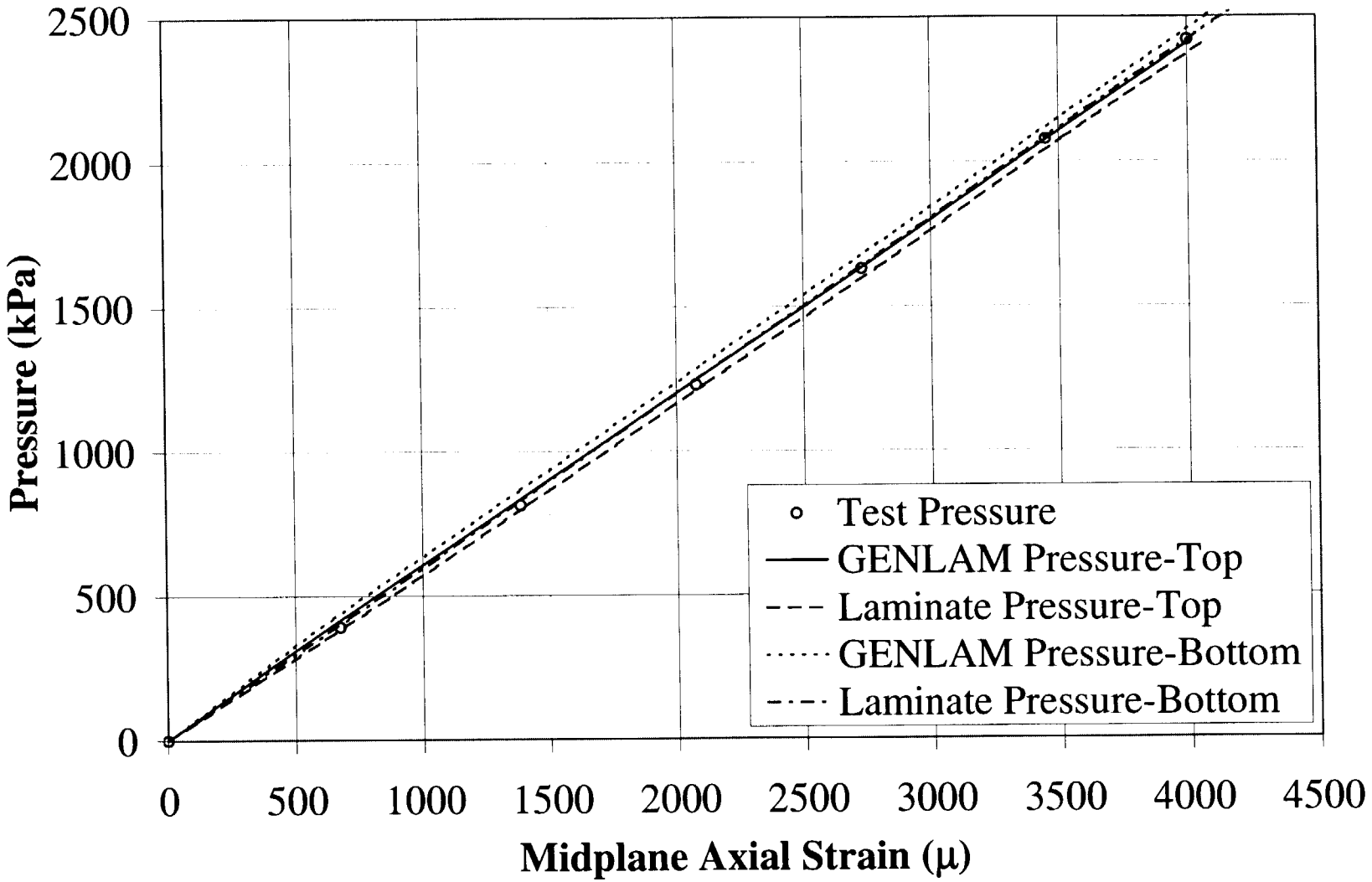

Figure 6 P1 Test Pressure versus Computer Analysis Pressure for Axial Strains

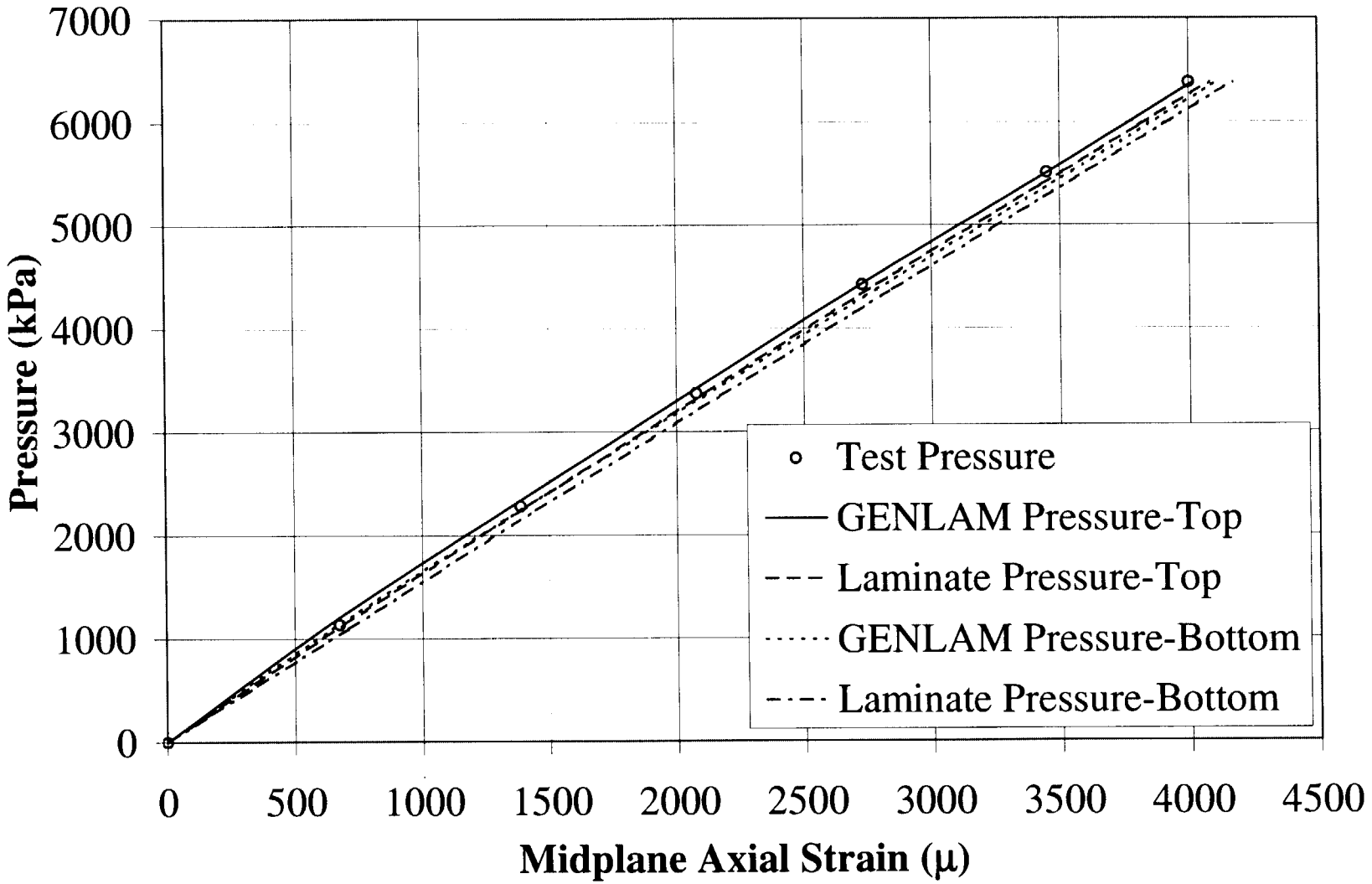

Figure7 P1 Test Pressure versus Computer Analysis Pressure for Hoop Strains

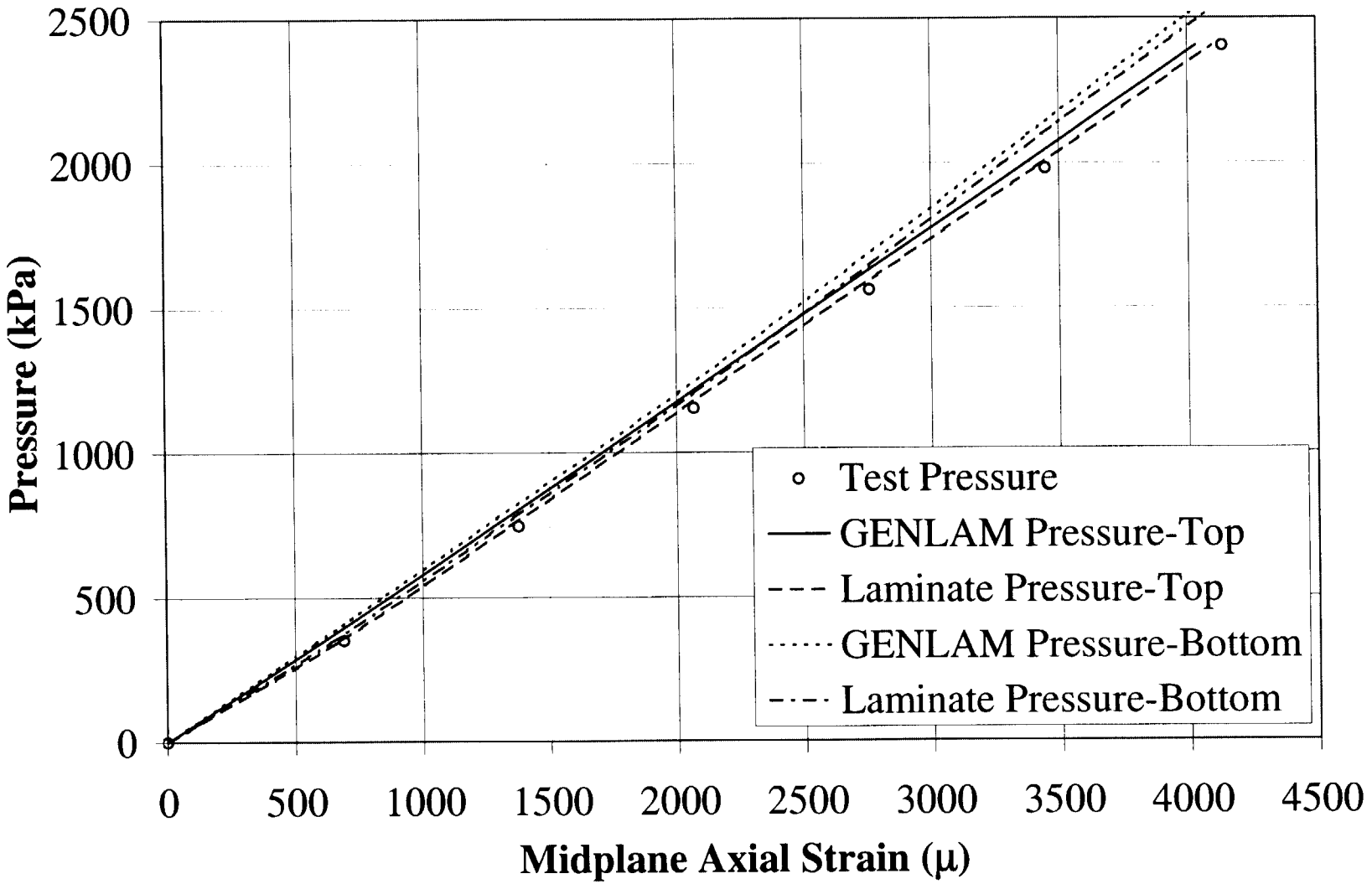

Figure 8 P2 Test Pressure versus Computer Analysis Pressure for Axial Strains

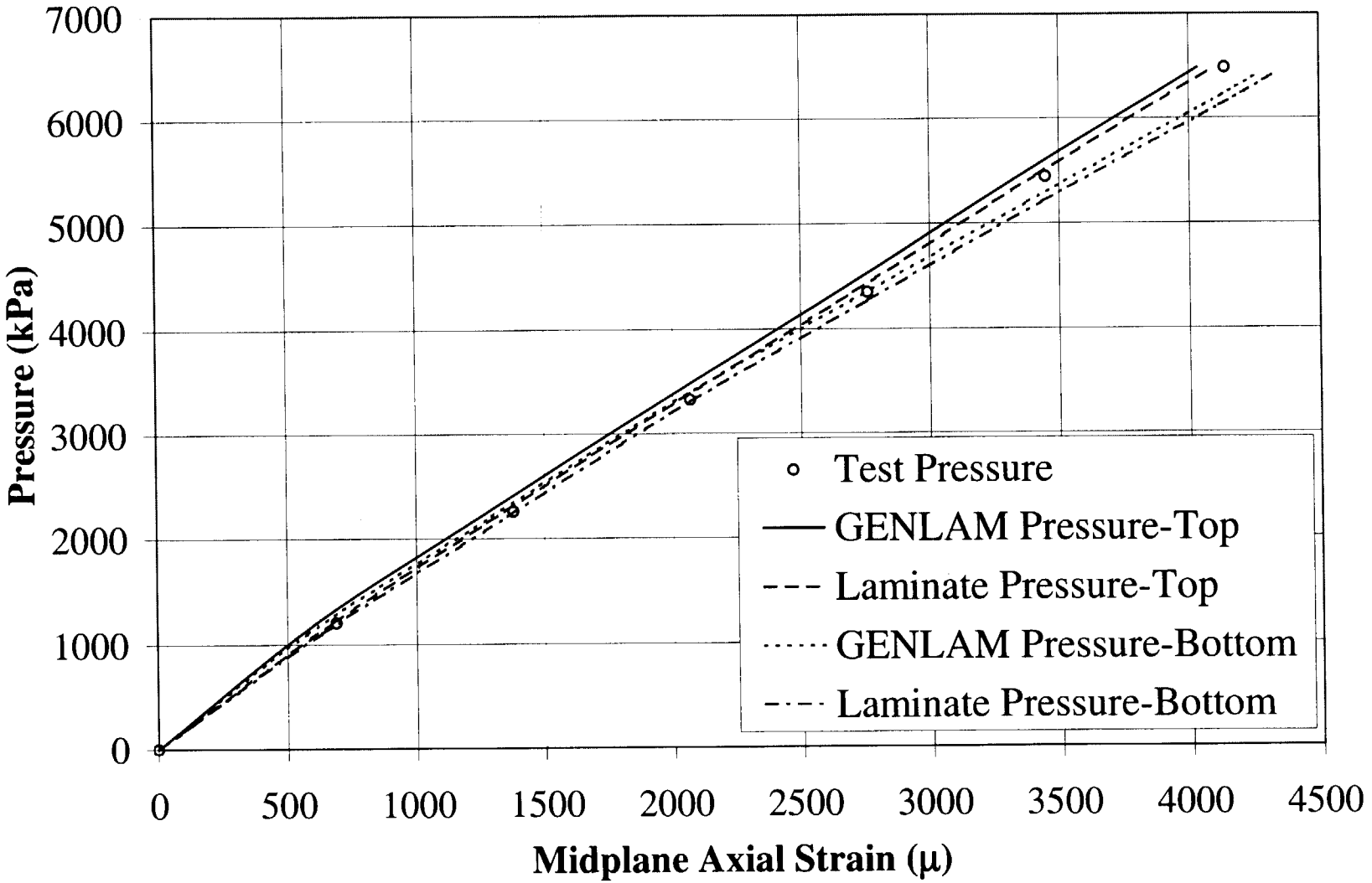

Figure 9 P2 Test Pressure versus Computer Analysis Pressure for Hoop Strains

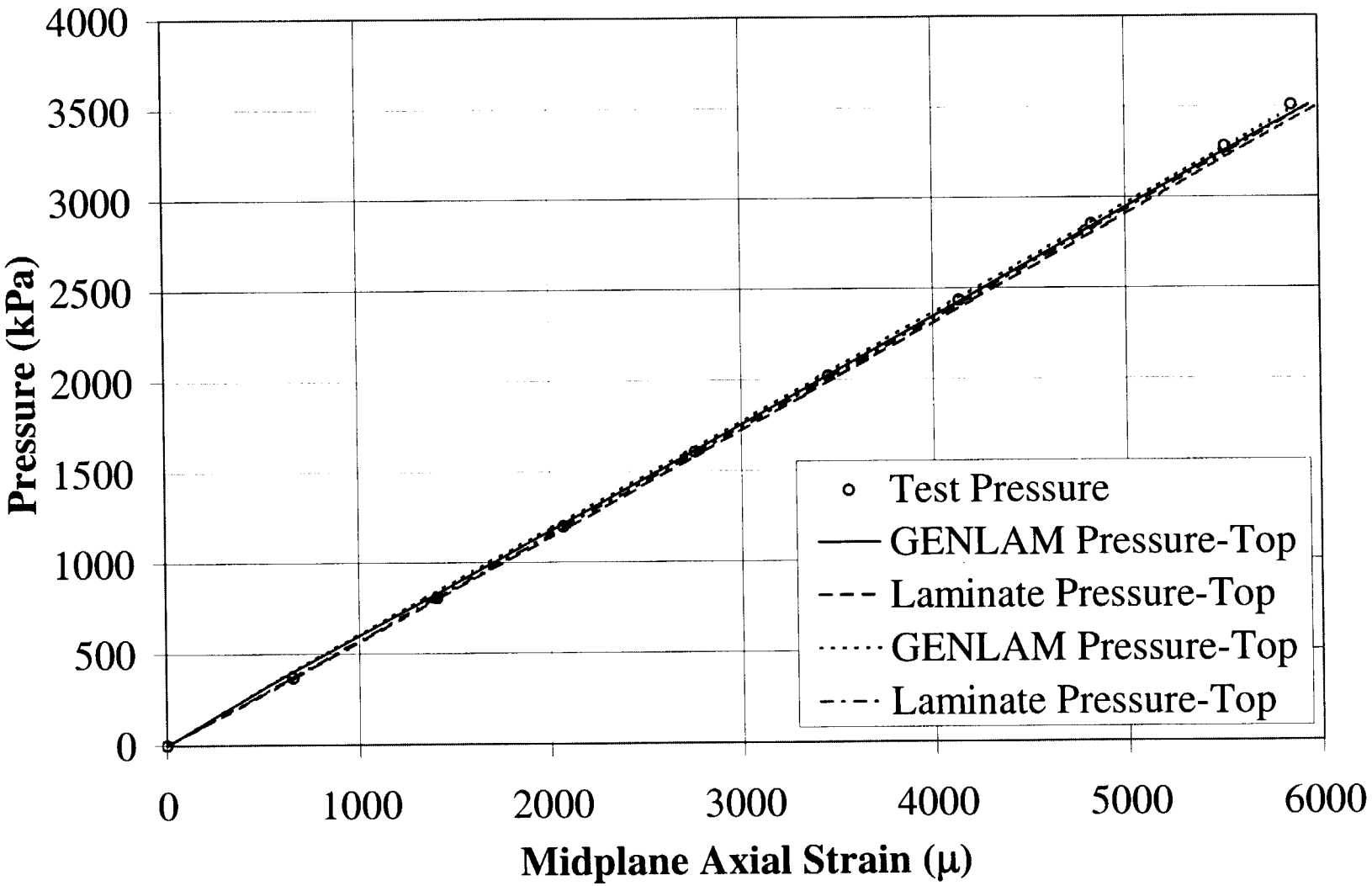

Figure 10 IP1 Test Pressure versus Computer Analysis Pressure for Axial Strains

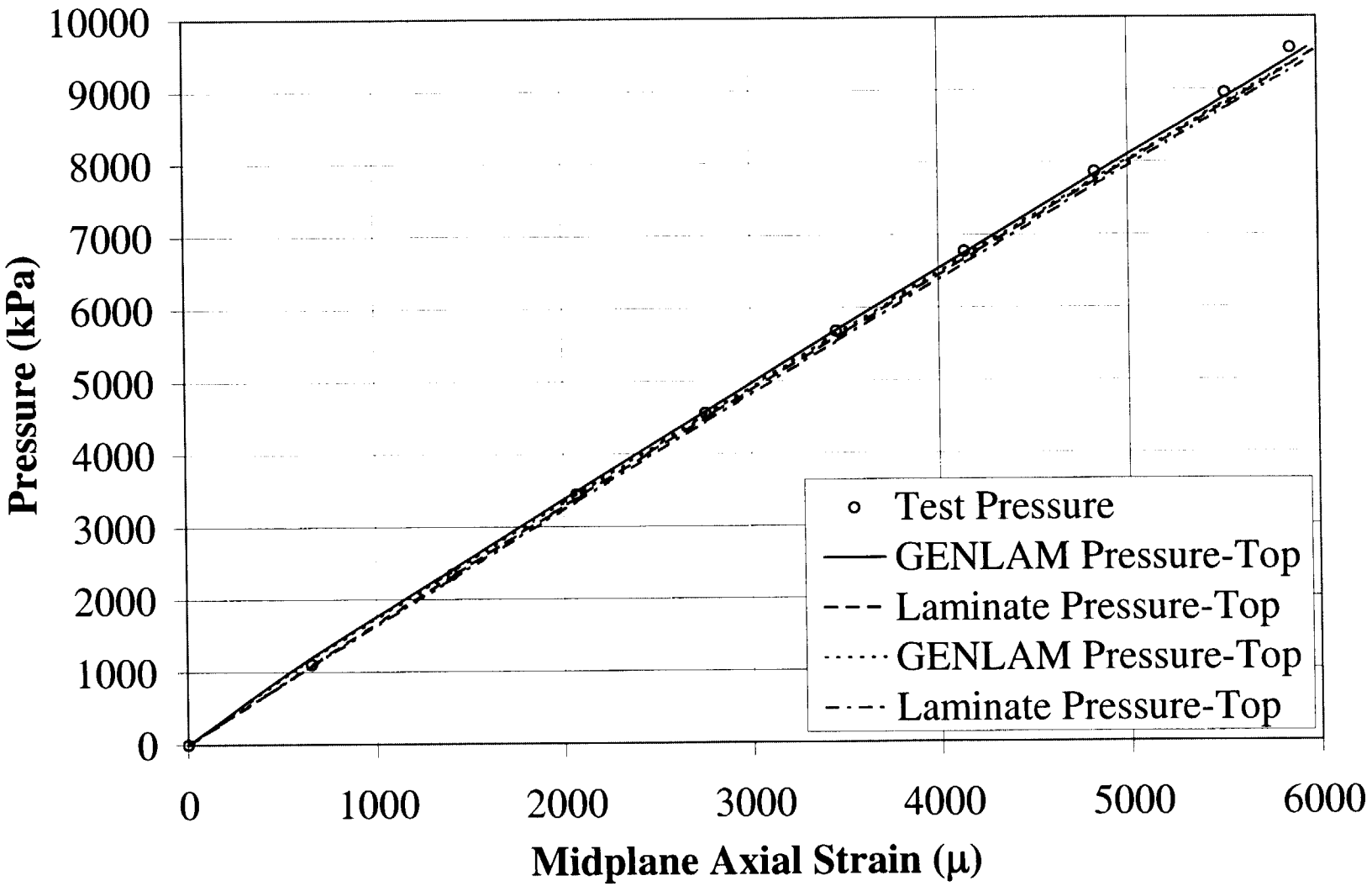

Figure 11 IP1 Test Pressure versus Computer Analysis Pressure for Hoop Strains

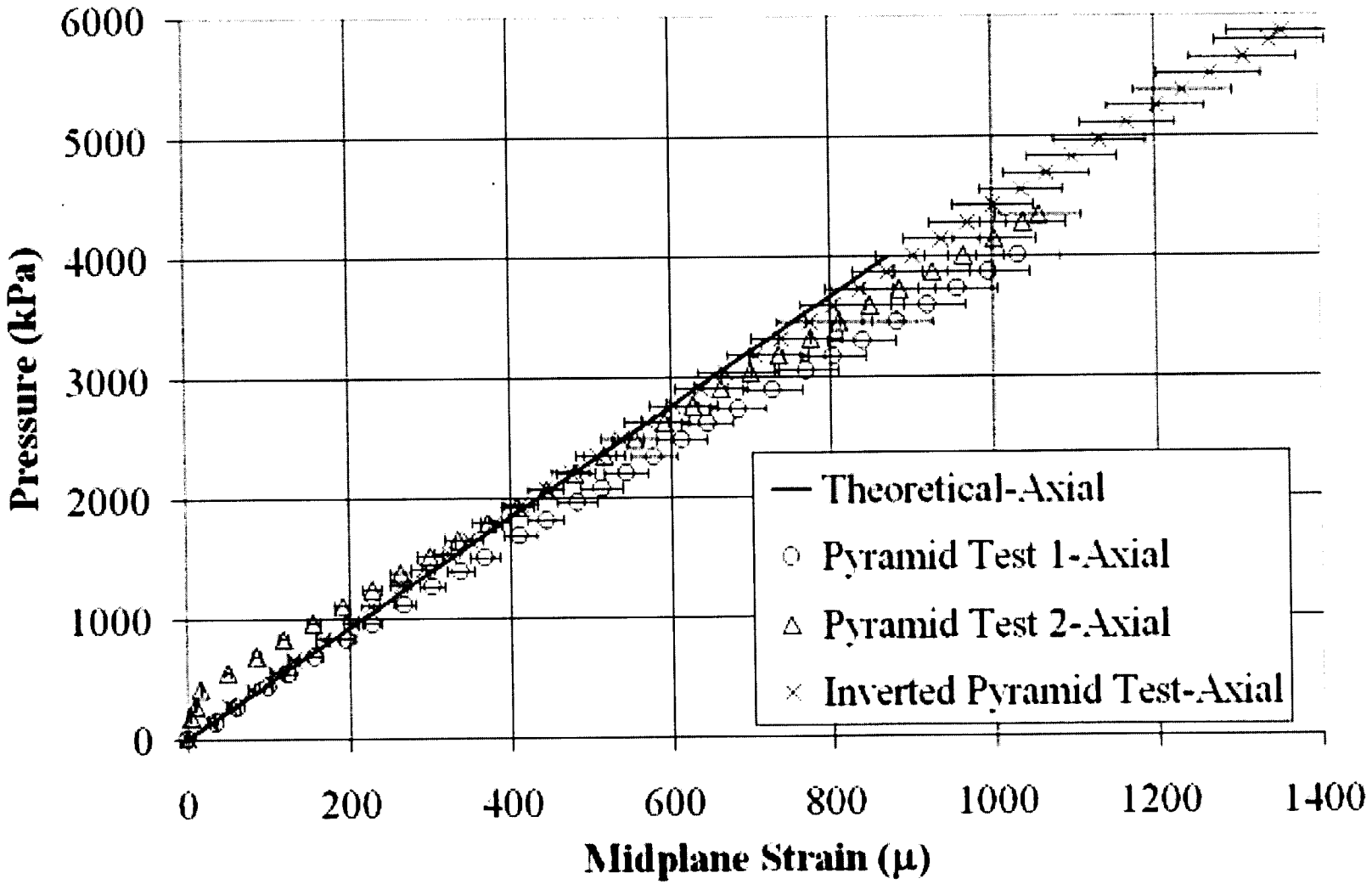

Figure 12 Axial Direction Joint Stiffness Test versus Analysis Results

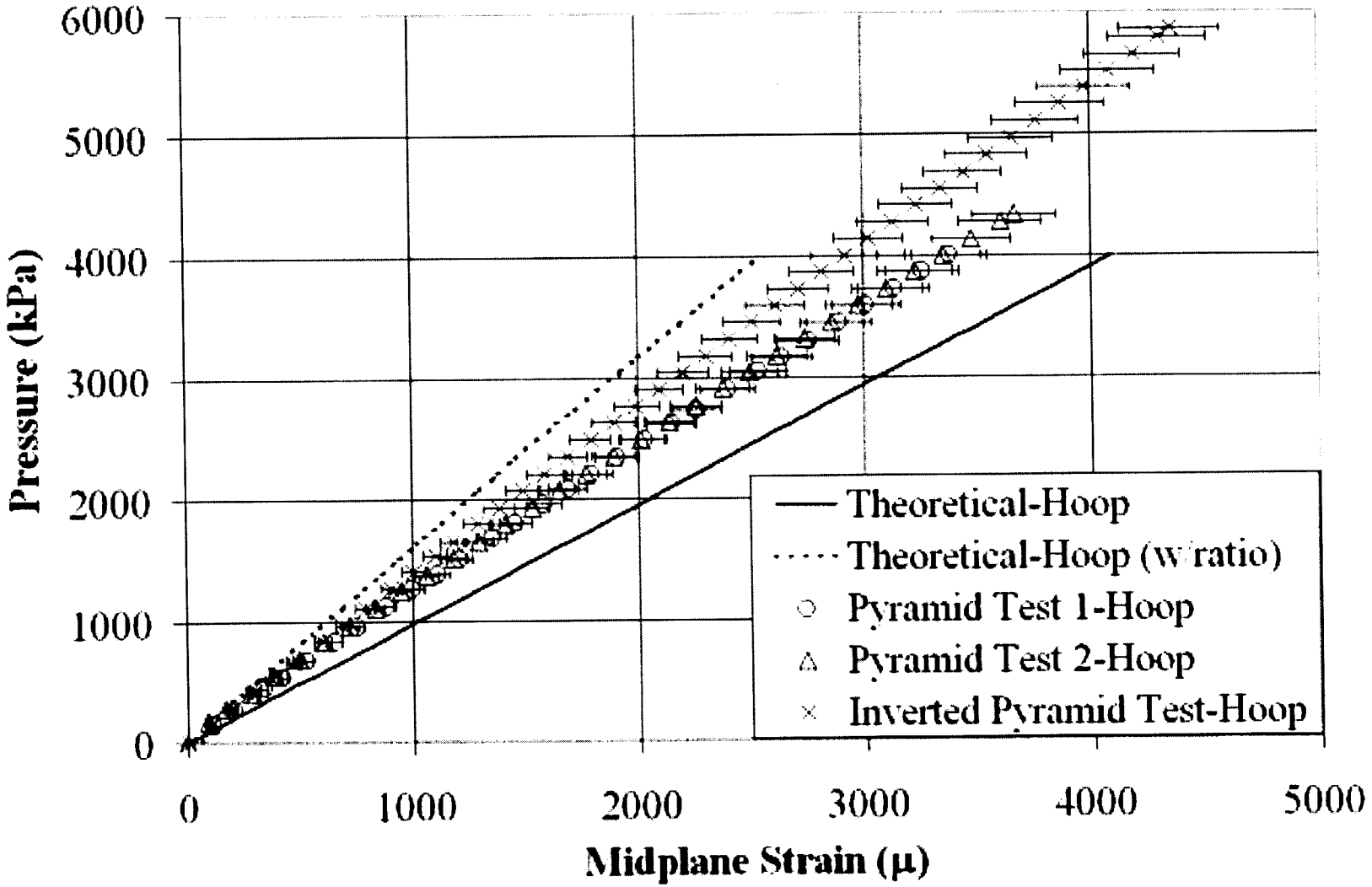

Figure 13 Circumferential Direction Joint Stiffness Test versus Analysis Results

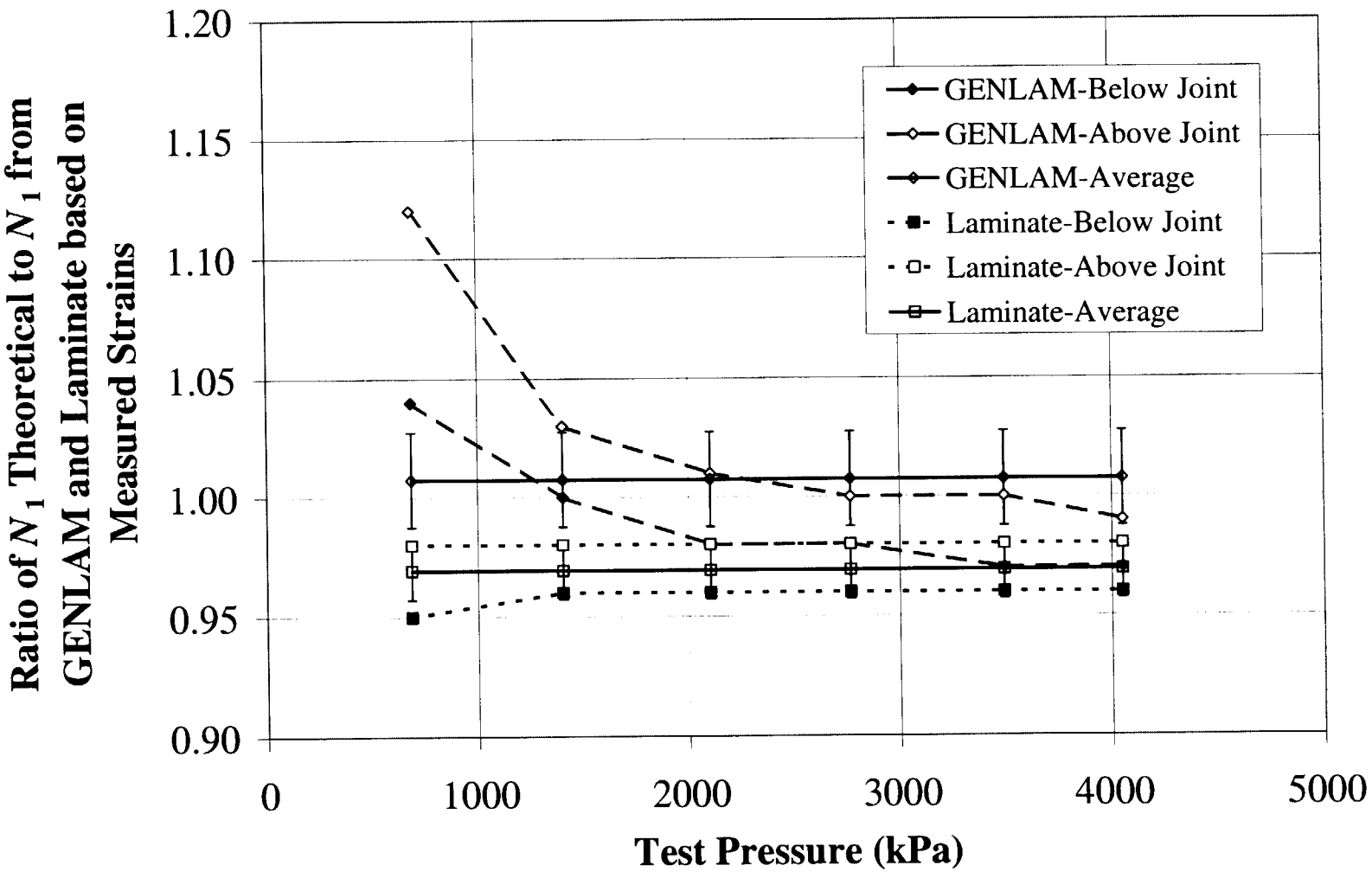

Figure 14 Comparison plot of the ratio of the theoretical value of the axial stress resultant versus that calculated from GENLAM and Laminate for the first Pyramid Joint Test.

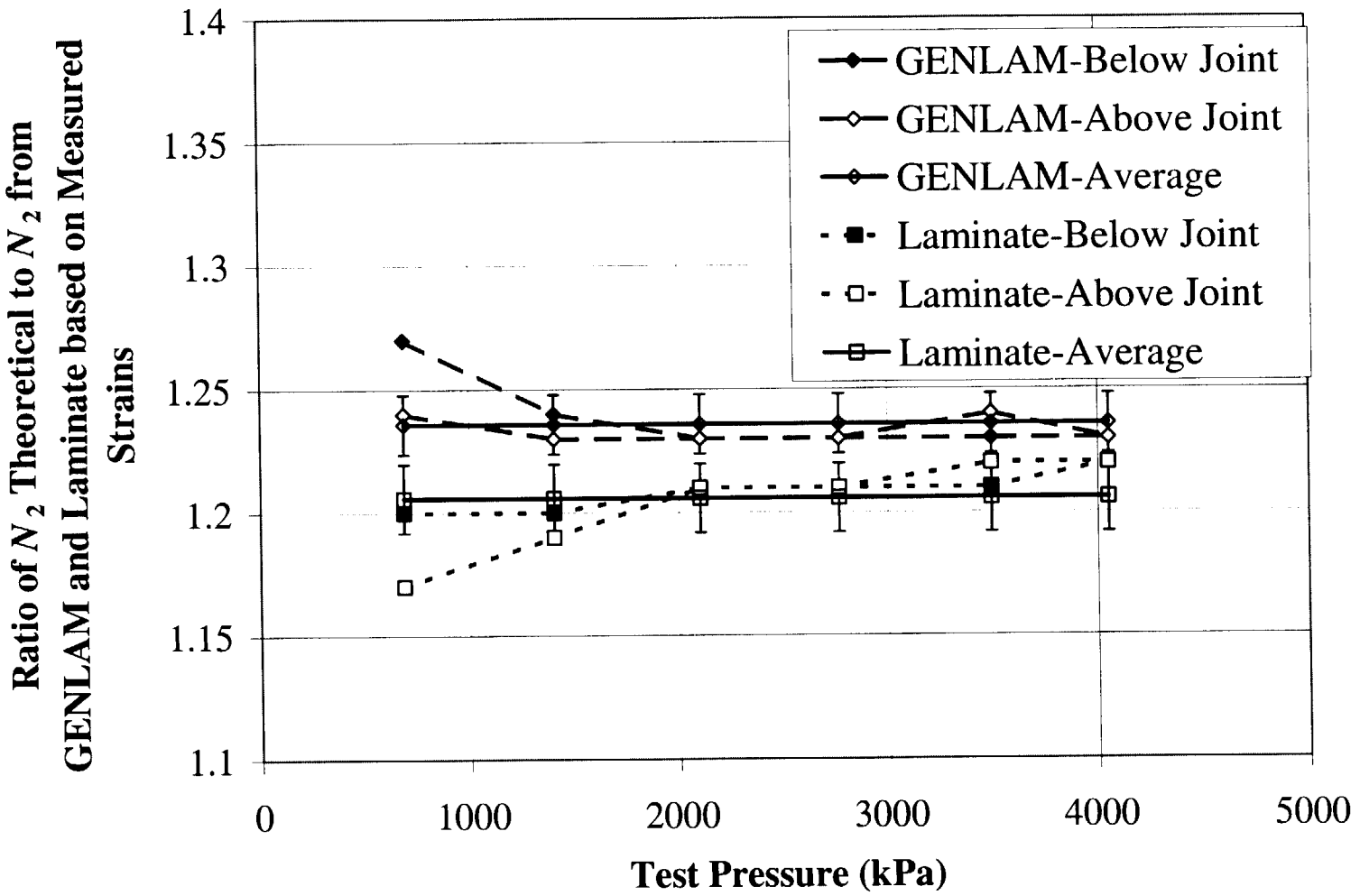

Figure 15 Comparison plot of the ratio of the theoretical value of the hoop stress resultant versus that calculated from GENLAM and Laminate for the first Pyramid Joint Test.

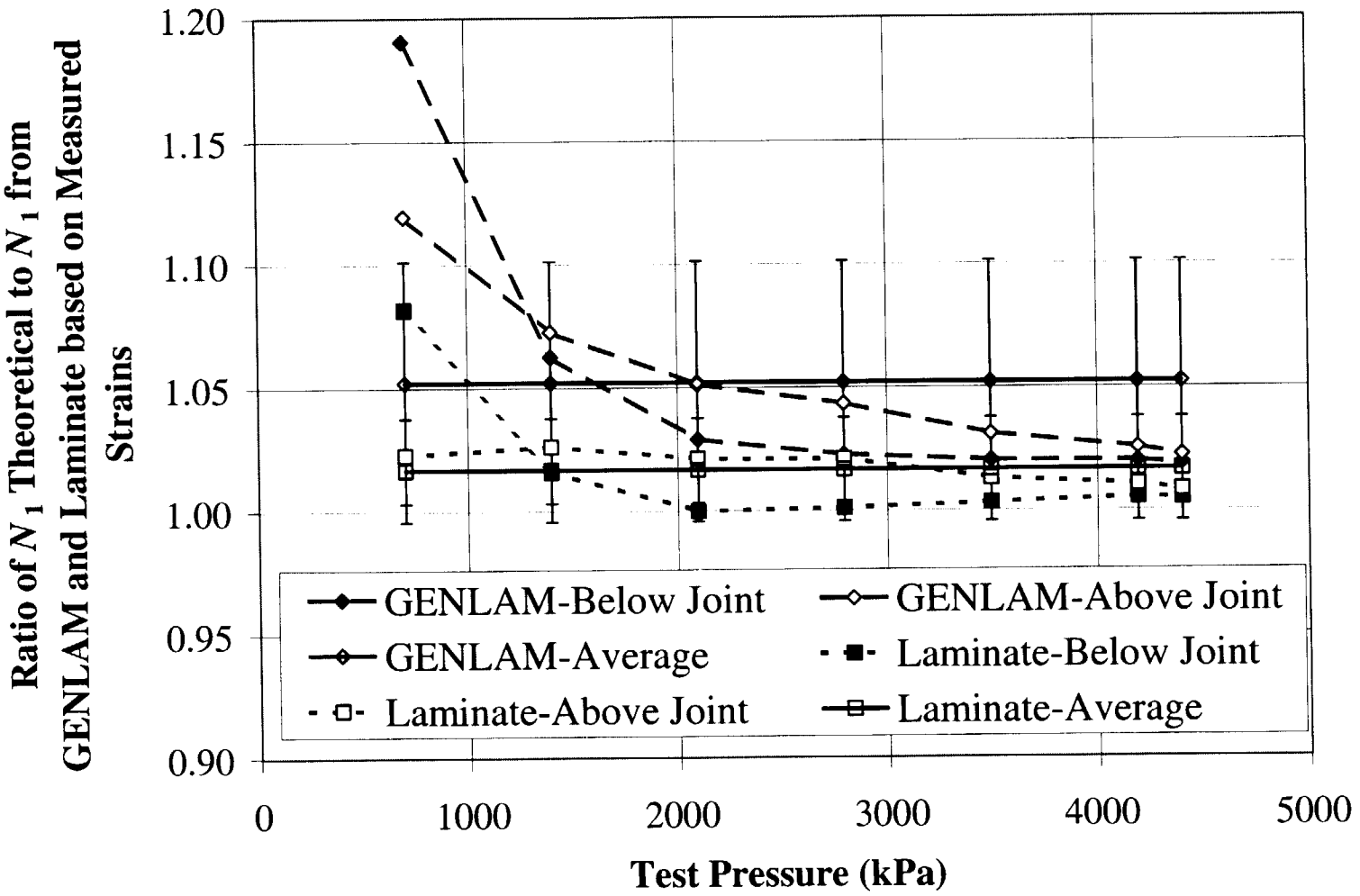

Figure 16 Comparison plot of the ratio of the theoretical value of the axial stress resultant versus that calculated from GENLAM and Laminate for the second Pyramid Joint Test.

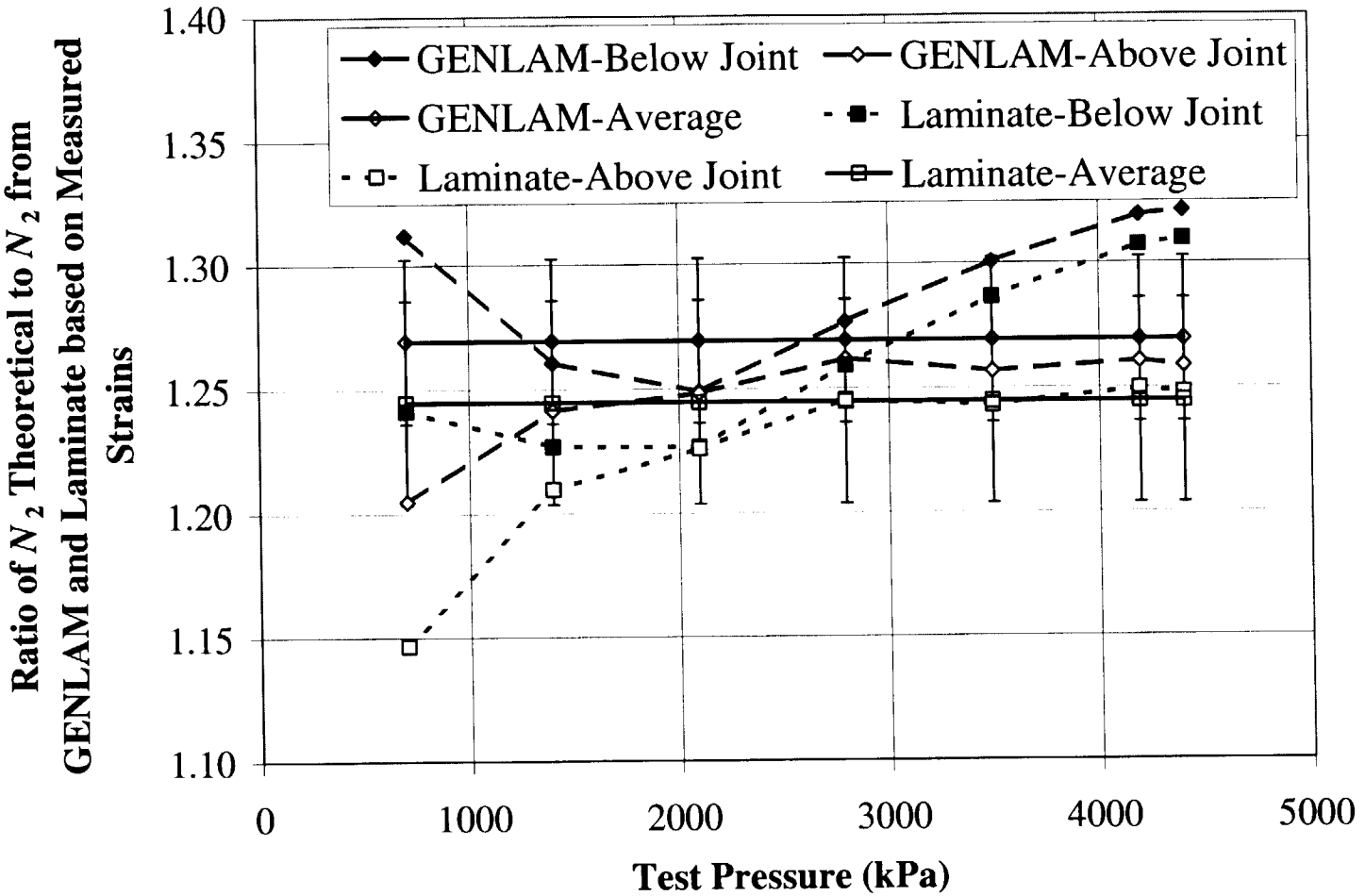

Figure 17 Comparison plot of the ratio of the theoretical value of the hoop stress resultant versus that calculated from GENLAM and Laminate for the second Pyramid Joint Test.

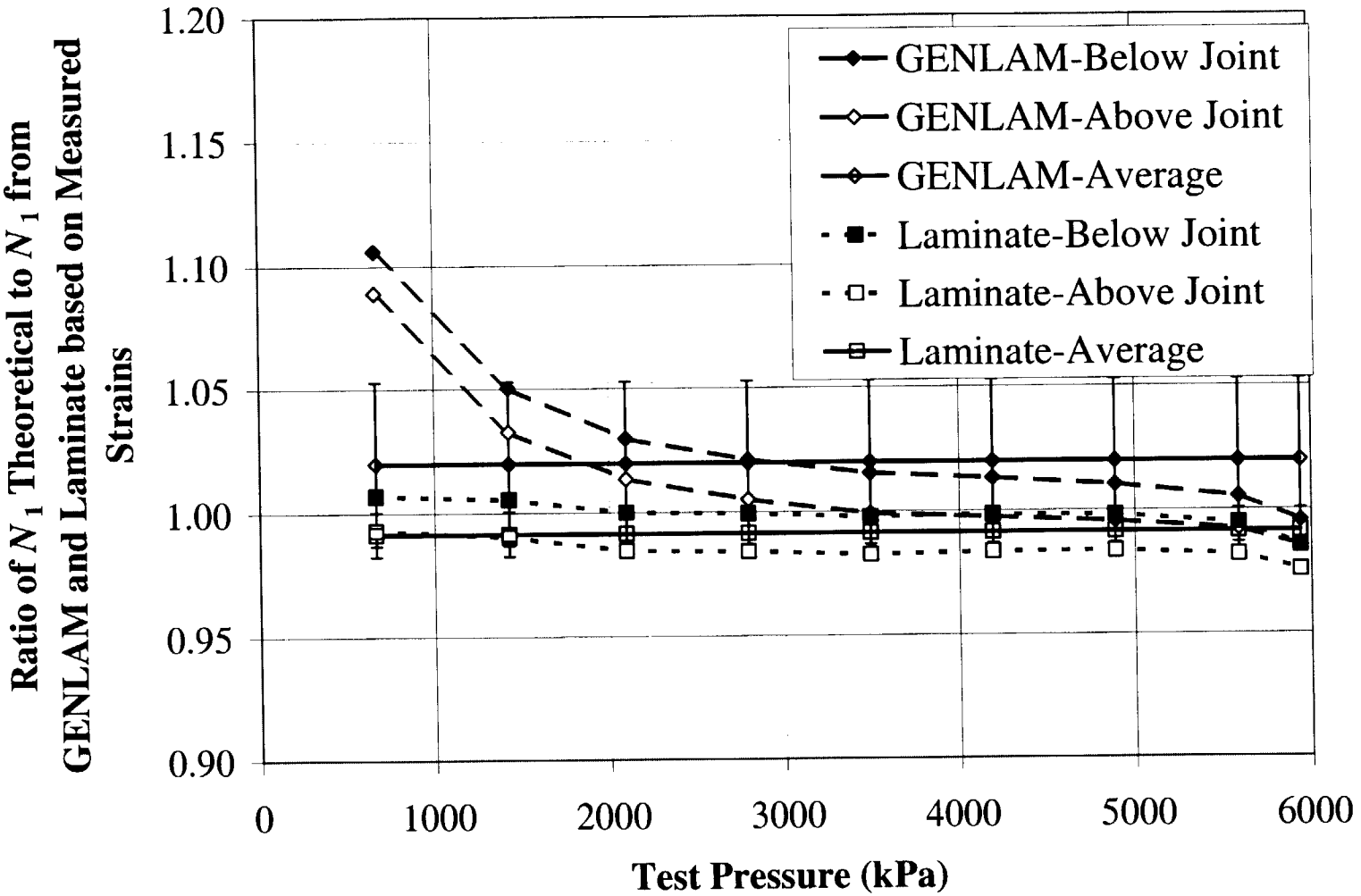

Figure 18 Comparison plot of the ratio of the theoretical value of the hoop stress resultant versus that calculated from GENLAM and Laminate for the Inverted Pyramid Joint Test.

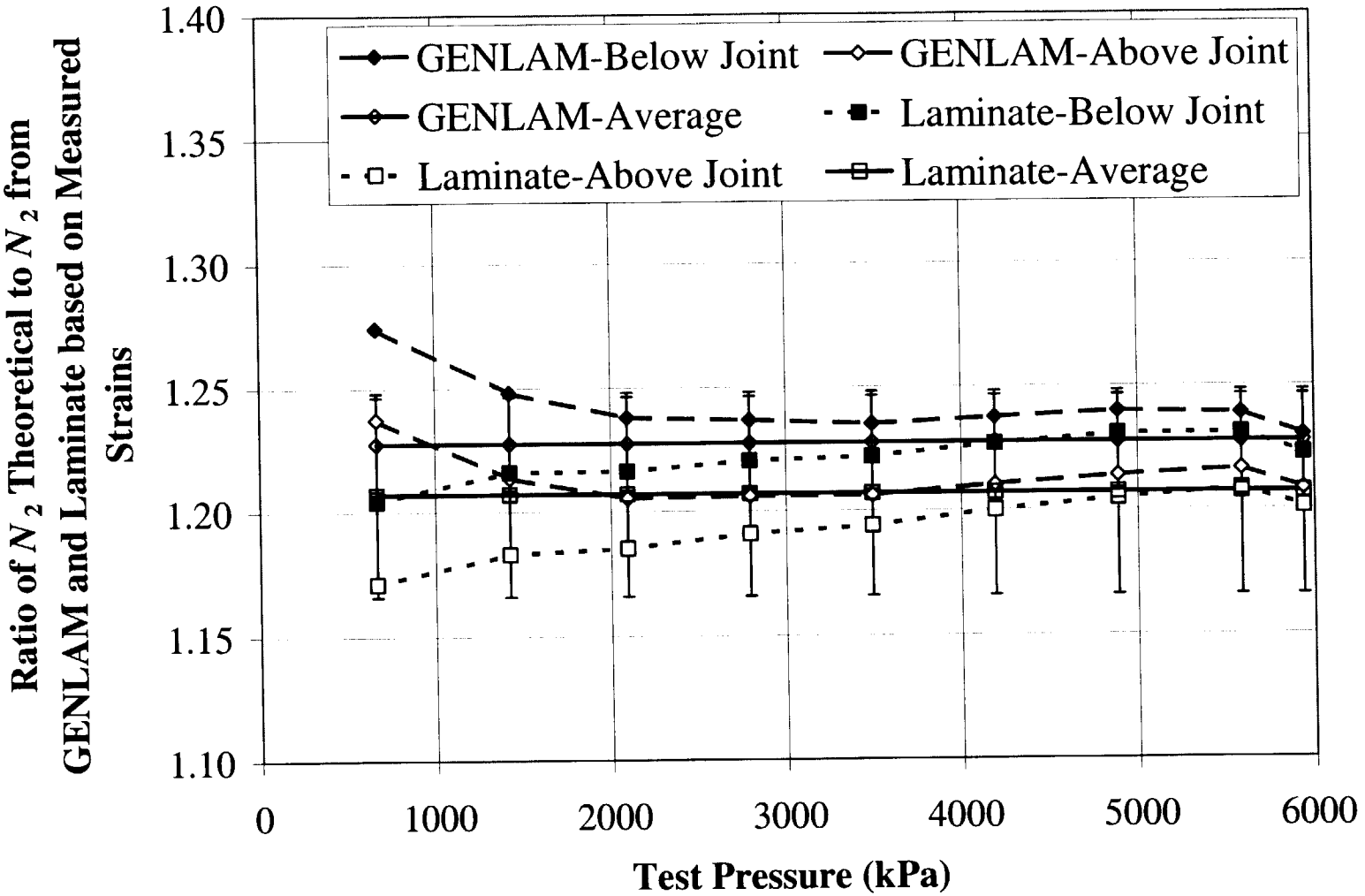

Figure 19 Comparison plot of the ratio of the theoretical value of the hoop stress resultant versus that calculated from GENLAM and Laminate for the Inverted Pyramid Joint Test.

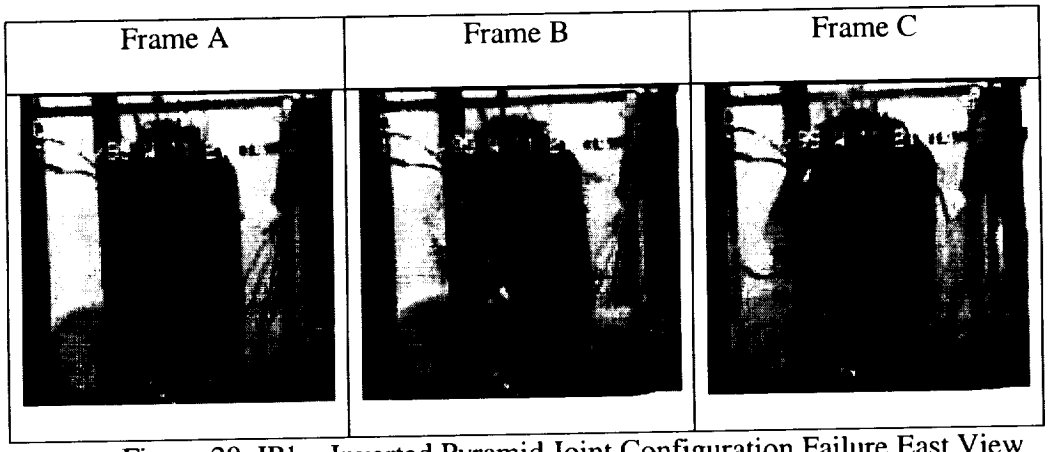

Figure 20 IP1 – Inverted Pyramid Joint Configuration Failure East View

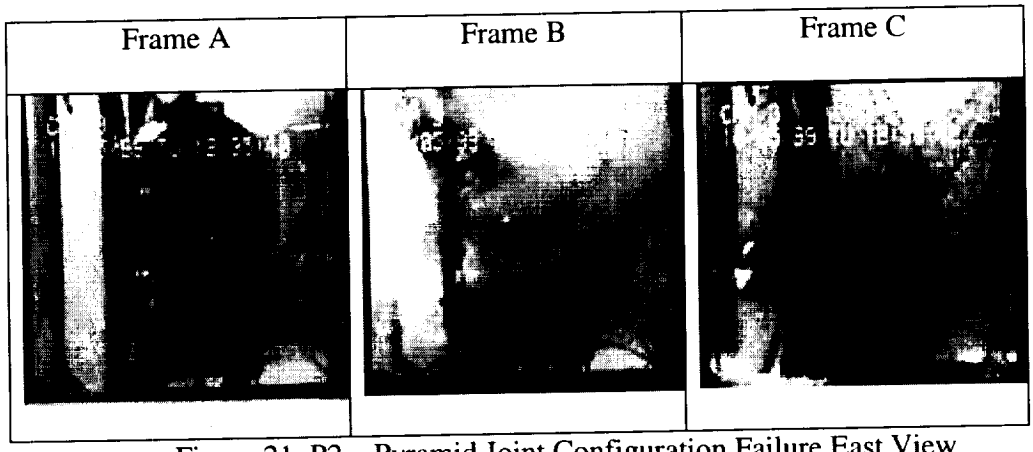

Figure 21 P2 – Pyramid Joint Configuration Failure East View

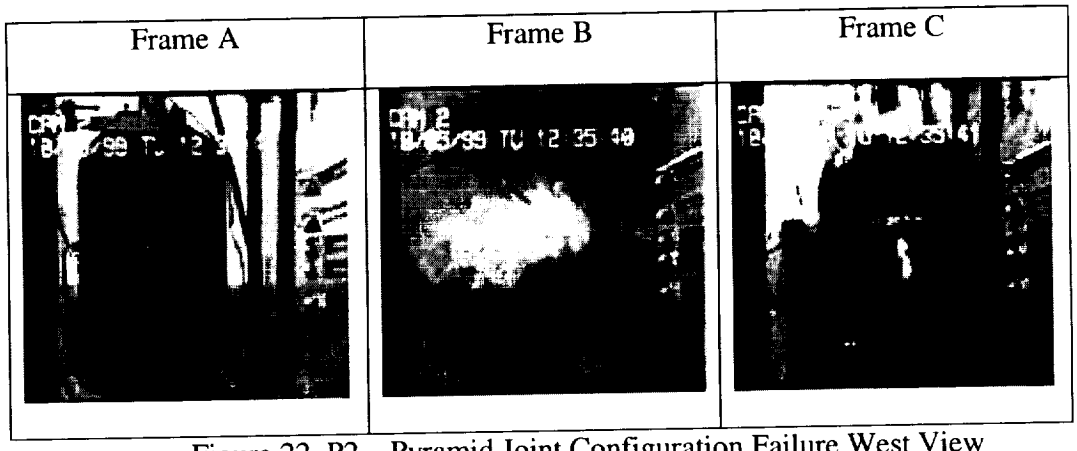

Figure 22 P2 – Pyramid Joint Configuration Failure West View